AN ABSTRACT OF THE THESIS OF

Chun Tsin Wang (Name) for the Doctor of Philosophy (Degree)

in METALLURGICAL ENGINEERING (Major) presented on August 14, 1970 (Date)

Title: DEFORMATION MECHANISM OF POLYCRYSTALLINE AND MONOCRYSTALLINE HIGH PURITY VANADIUM AT LOW TEMPERATURES

Abstract approved: Redacted for Privacy
Dr. Douglas W. Bainbridge

High purity vanadium, both in the polycrystalline and monocrystalline form, was strained in tension in order to study the controlling deformation mechanism at temperatures between 77 and 293°K. The temperature and strain rate dependence of the flow stress for two grades of material, 99.99% and 99.93%, was evaluated using temperature change and strain rate change procedures.

An abrupt change of yield and flow stresses, strain rate sensitivity, activation enthalpy and volume at approximately 200°K indicates that a change of rate controlling mechanism occurs at this temperature.

It was found that at temperatures below 200°K, the activation enthalpy is less than 1 ev. and the activation volume is less than 30 b^3. A high strain hardening rate

in the early stages of straining and an orientation dependence of flow stress were also noticed. Among all possible controlling activation processes, the pseudo-Peierls mechanism, i.e, the slightly dissociated screw dislocation model, agrees best with the observations.

In the temperature range from 200 to 293°K, the yield and flow stresses of vanadium were remarkably affected by the level of impurity content. On the basis of this observation, the controlling process in this temperature range is most probably the interaction between dislocations and impurities.

Mechanical twins were formed on single crystals at 77 and 120°K; twins occur on $\{211\}$ planes. Slip lines could not in general be identified, but were noted in one test. The slip plane determined on a single crystal with <110> axis deformed at 160°K was $\{211\}$. Single crystals generally showed a chisel edge type of ductile fracture.

Deformation Mechanism of Polycrystalline and Monocrystalline High Purity Vanadium at Low Temperatures

by

Chun Tsin Wang

A THESIS

submitted to

Oregon State University

in partial fulfillment of
the requirements for the
degree of

Doctor of Philosophy

June 1971

APPROVED:

Redacted for Privacy

Professor of Metallurgical Engineering

in charge of major

Redacted for Privacy

Head of Department of Metallurgical Engineering

Redacted for Privacy

Dean of Graduate School

Date thesis is presented August 14, 1970

Typed by Pat McCauley for Chun Tsin Wang

ACKNOWLEDGEMENTS

The author is very grateful to Dr. Douglas W. Bainbridge, under whose guidance and constant discussion this work was performed. He is also grateful to Professors W.D. McMullen, J.A. McComb, R.D. Olleman and O.G. Paasche for their helpful comments and discussions.

The author wishes to thank Dr. T.A. Sullivan of U.S. Bureau of Mines, Boulder City, Nevada, for kindly donating the electrorefined vanadium and providing a part of the chemical analysis of vanadium specimens.

Appreciation and hearty thanks are due Mr. Andy Van Echo of U.S. Atomic Energy Commission, Headquarters, Germantown, Maryland, who showed enthusiasm and encouragement and coordinated with this work so that the zoning of single crystals could be performed at the Oak Ridge National Laboratory. The same appreciation and thanks are to Mr. P.L. Rittenhouse and Dr. R.A. Reed of ORNL, who converted the vanadium rods into single crystals by electron beam float zone refining process using their excellant techniques and equipment.

The research was partially supported by Teledyne Wah Chang Corp., Albany, Oregon, to which the author would like to express his appreciation. Special thanks go to Messrs. S.W.H. Yih, S.A. Worcester, E.F. Baroch

and R.H. Nielsen. Among those who helped to work in the present investigation, Messrs. M.B. Siddall, M.M. Mills, J.V. Berry, R. D. Ayers, R.W. Griffin, W.E. Anable, W.C. McBee, C.D. Dysle, P.E. Danielson, J.L. Westling, J.I. Cosman and Mrs. M.J. Kappler and P.E. McCauley are gratefully acknowledged.

The thesis is dedicated to the memory of the author's parents, Teh Kwang and Cheng Wei-Y, and grandmother, Tsung Lao, who taught and persistantly encouraged him to strive for some academic achievement.

TABLE OF CONTENTS

LIST OF TABLES

LIST OF FIGURES

THE DEFORMATION MECHANISM OF POLYCRYSTALLINE AND MONOCRYSTALLINE HIGH PURITY VANADIUM AT LOW TEMPERATURES

I. INTRODUCTION

Vanadium, with an atomic number of 23 and a density of 6.1 gm per cm^3, belongs to Group V-A transition metals and possesses a body centered cubic crystalline structure. It has been well known as an alloying element for steel since 1896 (Tietz and Wilson, 1965), and widely used in aluminum and titanium industries in recent years. However, investigations relative to the deformation of vanadium have been scarce as compared to other BCC transition metals, e.g., niobium and tantalum of Group V-A, chromium, molybdenum and tungsten of Group VI-A and iron of Group VIII. This is probably, at least partially, attributed to the difficulties in obtaining the metal in a high purity form.

Vanadium has been commercially produced by aluminothermic or calcium reduction, which yielded the metal of the purity of from 80% to 95% and up to 99.8% respectively (Rostoker, 1958; Tietz and Wilson, 1965). The first successful attempt to produce ductile vanadium was reported by Van Arkel who used the iodide decomposition process and the product purity was approximately 99.9% (Carlson and Owen, 1961).

Recent findings that vanadium base alloys might be prospective fuel cladding materials for the next generation,

liquid metal cooled fast breeder reactors (Yaggee, Gilbert and Styles, 1969) have spurred interest in high purity vanadium preparations. The electrolytic refining process was then developed by Sullivan (1965) and the purity of the product ranged from 99.9% to 99.99%. Carlson, Schmidt and Krupp (1966) combined the processes of aluminothermic reduction under inert atmosphere, high temperature sintering and electron-beam melting and were able to produce a product of greater than 99.9% purity. Wang et al. (1970) modified the process and scaled up the production with a final product of 99.93% purity.

The body-centered cubic transition metals have broadly similar deformation characteristics, although there are differences in some respects. It is relatively easy to purify the Group V-A metals, vanadium, niobium and tantalum to ensure ductile behavior at low temperatures, but very difficult to do this with the Group VI-A metals chromium, molybdenum and tungsten. This difference seems to arise from the equilibrium solubilities of usual interstitial solutes, which are high for Group V metals and very low for Group VI metals, but it may also be related to the dislocation dynamics. An important factor in maintaining ductility when the yield stress becomes high is the ability to blunt a crack by local plastic deformation, and this depends on dislocation mobilities and dislocation multiplication rates. A further difference between the

Group V and Group VI metals is that the former have a low work-hardening rate, while the latter work harden more readily at low temperatures. The characteristics of iron seem to be intermediate between the two groups.

The general deformation characteristics common to all BCC transition metals are as follows: (1) indistinctive and controversial slip systems; (2) twinning at very low temperatures; (3) strong temperature dependence of the yield and flow stresses at sub-ambient temperatures and the probability that this is due to a common deformation mechanism.

The aim of the present work is to investigate the deformation characteristics mentioned above by using high purity vanadium and the emphasis will be placed on the origin of the deformation mechanism in the low temperature range. Two grades of polycrystalline material and two orientations of single crystals were used in order to study the effect of impurities and orientation on the mechanism.

II. THEORETICAL BACKGROUND

(A) Slip and Twin Systems in BCC Metals

In most metals the planes on which slip takes place are usually those with quite dense atomic packing and the slip direction is almost always the most closely packed direction in the plane. In the hexagonal close-packed structure the basal plane $\{0001\}$ is the closest-packed plane, which is the common slip plane in cadmium, magnesium and zinc. However, slip on prismatic plane $\{10\bar{1}0\}$ has also been observed frequently in HCP metals (Honeycombe, 1968).

The face-centered cubic metals, e.g., aluminum, copper, gold, nickel, and silver, deform primarily on the close-packed octahedral $\{111\}$ planes in the <110> close-packed directions. Except for aluminum at high temperatures, it is rare to find a slip plane other than one of the octahedral planes (Honeycombe, 1968).

The body-centered cubic metals present a somewhat more complicated and controversial picture. Although, in general, they all slip in the closest-packed <111> direction, the choice of slip plane varies greatly. The planes with the common zone axis <111> are, in order of density, with which the atoms are packed, $\{110\}$, $\{112\}$ and $\{123\}$ planes. In fact, all these planes and the maximum resolved shear stress plane have been reported to be operative slip

planes for iron, niobium, tantalum, molybdenum and tungsten (Table 1). Recent investigations in niobium (Foxall, Duesbery and Hirsch, 1967) revealed that the slip system is dependent upon orientation but the Schmid Law is not obeyed. Due to the dissociation of a <111> type screw dislocation on {112} planes, there are hard and soft directions for which different resolved shear stresses are required for the slip system to be operative.

Twinning, which involves a small but well defined volume within the crystal, is accompanied by energy release in the form of sound, e.g., the cry of tin. The twinned region is often bounded by parallel crystalline planes, called twin habit planes or twinning planes.

While twinning is not a dominant mode of deformation in metals which possess many possible slip systems, e.g., FCC metals, it is very significant in metals where the possible slip systems are severely limited, e.g., the HCP metals.

Mechanical twins form more readily in BCC metals as the rate of deformation is increased; the tendency to twin increases with decreasing temperatures and increasing purity of the metal (McHargue, 1962).

Twins have been found in iron (Kelly, 1953), molybdenum, tungsten (Schadler, 1960), chromium, niobium (McHargue, 1962) and tantalum (Barrett and Bakish, 1958).

TABLE 1

SLIP PLANES OBSERVED IN BCC METALS

METAL	{110}	{211}	{321}	MRSS*	TEMP. (°K)	REFERENCE
Fe				x	293	Taylor and Elam (1926)
Fe				x	293	Jaoul and Gonzalez (1961)
Fe	x	(x)	(x)	x	293	Barett, Ansel and Mehl (1937)
Fe	x	x			293	Stein and Gorsuch (1961)
Nb	x	x			293	Taylor (1965)
Nb	x	x			293	Duesbery and Foxall (1965) (high purity)
Nb	x	x	x		293	Duesbery and Foxall (1965) (low purity)
Nb	x x	x x	(x) (x)	(x) (x)	293, 158	Bowen, Christian and Taylor (1967)
Ta	x	x			293	Mordike (1961)
Ta				x	>77	Mitchell and Spitzig (1965)
Mo		x x			293; 573	Tsien and Chow (1937)
Mo	x	x	x		293	Maddin and Chen (1954)
Mo	x	x	x	x	293	Hoke and Maddin (1956)
W	x	x			<293	Garlick and Probst (1964)
W	x		x		293	Kaun et al. (1965)
W	x x				77, 20	Schadler (1960)
V		x x			77, 298	Greiner and Boulin (1967)
V	x x				77, 500	Mitchell, Fields and Smialek (1970)

* The plane of maximum resolved shear stress; it is usually a non-crystallographic plane.

The twinning plane is in most cases, $\{112\}$ and the shear displacement, 1/2a <111>, which is unidirectional. To produce a twinned crystal the operation must be carried out on each successive (112) plane to produce the stacking sequence ABCDEFEDCBA; the shear strain produced is 0.707. Due to the fact that a large shear strain is associated with twinning in BCC metals, and a large amount of energy is required to nucleate twins, they are usually long and thin, rarely thicker than 5×10^{-4}cm (Honeycombe, 1968).

(B) Yield Point Phenomena in BCC Metals

It has been generally accepted that the presence of interstitial atoms or precipitates has a large effect on the yield phenomena in BCC metals. This is mainly caused by the interaction of the strain fields associated with dislocations and nearby impurity atoms (Cottrell and Bilby, 1949). If this interaction reduces the total free energy of the crystal then the stress required to move the dislocation is increased. After unlocking, and tearing dislocations from their pinning points, the stress drops sharply from the upper yield point to the lower yield point, where the yield elongation occurs and a Lüders band runs through the material at roughly constant stress. However, recent investigations seem to show that the temperature dependence of the yield point is not due to pinning but is caused by a strong frictional stress acting on unpinned dislocations.

For example, the effect of grain size, with diameter d, on the lower yield stress, σ_y is experimentally found to be $\sigma_y = \sigma_i + kd^{-\frac{1}{2}}$ where σ_i has been interpreted as a frictional stress acting on free dislocations and k is proportional to the stress to unlock dislocations (Cotrell, 1958). Heslop and Petch (1956) have shown that in α-iron the frictional stress σ_i is strongly temperature dependent. It has been also shown that if this interpretation of the grain size effect on the yield stress is correct, then the locking stress in α-iron is practically temperature independent at temperatures between 110°K and 300°K. Therefore, in this temperature range the temperature dependence of yield stress is almost exclusively due to the frictional stress. Furthermore, it has been shown that the temperature dependence of the flow stress is the same as that of the yield stress and that the thermal component of the flow stress is independent of strain (Conrad and Schoeck, 1960). The flow stress cannot be governed by an unlocking mechanism at ambient and lower temperatures where the pinning points are essentially stationary.

These difficulties direct attention to an alternative view developed by Gilman and Johnston (1957). Their studies show that LiF crystals exhibit a prominent yield drop. Yet they find no evidence of unlocking. Grown in dislocations remain locked. Dislocations responsible for

slip are heterogeneously nucleated and multiply rapidly. Johnston and Gilman (1959) account for the yield point drop quantitatively simply in terms of the rapid multiplication of dislocations and the stress dependence of dislocation velocity.

One mechanism which could produce large numbers of dislocations and would be in accord with observations on silicon-iron is the double cross-slip mechanism (Low and Guard, 1959) originally proposed by Koehler (1952).

The overall picture of yielding may be explained as follows: During the initial loading of the specimen, some dislocations are torn from their Cottrell atmosphere at regions of stress concentrations. As the stress is increased their mobility increases and some multiplication occurs by the double cross slip mechanism. This gives the preyield microstrain. At a critical stress, first reached near the specimen grips and representing the upper yield stress, suddenand profuse multiplication occurs giving a Lüders band. At the lower yield stress this multiplication continues at the stress concentration existing at the band front. Once the Lüders band has traversed the length of the specimen, the number of dislocations contributing to the deformation remains essentially constant. However, the total density continues to increase because some dislocations are becoming stuck or entangled giving strain hardening. (Conrad, 1961).

(C.) The Physical Origin of the Thermal Component of the Shear Stress

The yield or flow shear stress of mechanical deformation consists of two parts: an athermal component τ_i which is the result of long range internal stress field for a given structure and is proportional to the shear modulus; and a thermal component τ^* which depends sensitively on temperature and strain rate.

To determine the physical origin of the thermal component of the shear stress, it is generally necessary to treat the problem as a thermally activated process. Assuming that a single activation process is rate controlling, the shear strain rate will be given by the expression,

$$\dot{\gamma} = NAb\nu \tag{1}$$

where N is the density of points of activation per cm^3; A is the area swept by the dislocation in one activated jump; b is the Burger's vector; and ν is the frequency of activation which is related to the atomic frequency ν_0 as follows:

$$\nu = \nu_0 \exp\left(-\frac{\Delta G}{kT}\right) \tag{2}$$

where ΔG is the free energy of activation, k, Boltzmann's constant and T, the absolute temperature (Christian and Masters, 1964). The activation energy is therefore,

$$\Delta G = -kT \ln \frac{\dot{\gamma}}{NAb\nu_0} \tag{3}$$

Assume $C = NAbV_o$ and ΔS is the activation entropy and both terms are independent of stress and temperature. Suppose the enthalpy of activation, ΔH is a function of temperature and the thermal component of the shear stress. We have,

$$\Delta H = \Delta H(T, \tau^*) \tag{4}$$

Differentiating Equation (3) with respect to temperature gives

$$\left(\frac{\partial \Delta G}{\partial T}\right)_{\dot{\gamma}} = \left(\frac{\partial \Delta G}{\partial T}\right)_{\tau^*} + \left(\frac{\partial \Delta G}{\partial \tau^*}\right)_T \left(\frac{\partial \tau^*}{\partial T}\right)_{\dot{\gamma}} \tag{5}$$

Therefore,

$$\Delta G = T\left(\frac{\partial \Delta G}{\partial T}\right)_{\tau^*} + T\left(\frac{\partial \Delta G}{\partial \tau^*}\right)_T \left(\frac{\partial \tau^*}{\partial T}\right)_{\dot{\gamma}} \tag{6}$$

Differentiating Eq. (3) with respect to $\ln \frac{\dot{\gamma}}{C}$ gives

$$\left(\frac{\partial \Delta G}{\partial \ln \frac{\dot{\gamma}}{C}}\right)_T = \left(\frac{\partial \Delta G}{\partial \tau^*}\right)_T \left(\frac{\partial \tau^*}{\partial \ln \frac{\dot{\gamma}}{C}}\right)_T = -kT \tag{7}$$

Substituting $\left(\frac{\partial \Delta G}{\partial \tau^*}\right)_T$ obtained from Eq. (7) into Eq. (6), we obtain

$$\Delta G = -kT^2 \left\{ \frac{\left(\frac{\partial \tau^*}{\partial T}\right)_{\dot{\gamma}}}{\left(\frac{\partial \tau^*}{\partial \ln \frac{\dot{\gamma}}{C}}\right)_T} \right\} + T\left(\frac{\partial \Delta G}{\partial T}\right)_{\tau^*} \tag{8}$$

Since in general

$$\left(\frac{\partial \Delta G}{\partial T}\right)_{\tau^*} = -\Delta S$$

it follows from Eq. (8), (Conrad and Wiedersich, 1960), that

$$\Delta H = -kT^2 \left\{ \left(\frac{\partial \tau^*}{\partial T}\right)_{\dot{\gamma}} \Big/ \left(\frac{\partial \tau^*}{\partial \ln \frac{\dot{\gamma}}{C}}\right)_T \right\} \tag{9}$$

Using the similarity between the thermodynamical pressure and the thermal component of shear stress, we have the activation volume

$$\Delta V = -\left(\frac{\partial \Delta G}{\partial \tau^*}\right)_T = kT \Big/ \left(\frac{\partial \tau^*}{\partial \ln \frac{\dot{\varepsilon}}{c}}\right)_T \qquad (10)$$

A common type of thermal activation barrier may be depicted as in Fig. 1 (Conrad, 1964). Upon application of an effective stress τ^*, the dislocation moves up the force barrier to the position F given by $F = \tau^* b \ell^*$ where b is the Burgers vector, and ℓ^* is the length of dislocation segment involved in the thermal activation. The energy which must be supplied by thermal fluctuations to overcome the obstacle is given by the shaded area under the curve and is designated by ΔG. The work done by the applied stress during thermal activation is

$$W = \tau^* b \ell^* d^* \qquad (11)$$

where $d^* = x_2 - x_1$, and $b \ell^* d^* = \Delta V$ (12)

while the activation free energy

$$\Delta G = \Delta G^* - b \ell^* \tau^* (x_2 - x_1)$$
$$= \int_{F = \tau^* b \ell^*}^{F_{max}} [x_2(F) - x_1(F)]\, dF \qquad (13)$$

where x is expressed as a function of F.

If F (x) is not a function of τ^*,

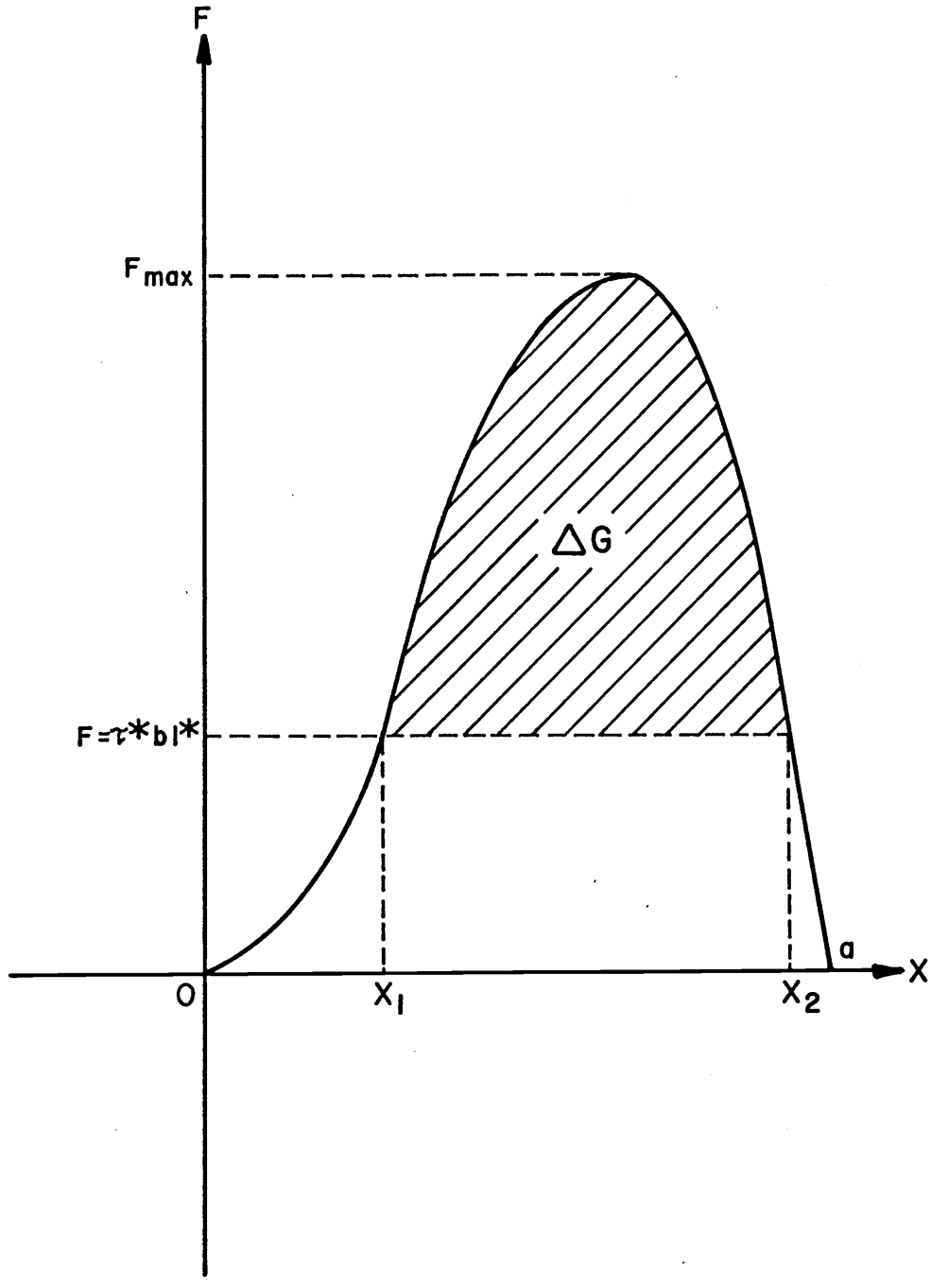

Fig. 1: Schematic diagram of the force-distance relationship for yielding or flow in BCC metals (Conrad, 1964).

differentiation of Eq. (13) with respect to τ^* gives

$$-\left(\frac{\partial \Delta G}{\partial \tau^*}\right)_T = (x_2 - x_1)\, b l^* \qquad (14)$$

From Eq. (10) and Eq. (14) we obtain

$$\Delta V = b l^* d^* = kT \Big/ \left(\frac{\partial \tau^*}{\partial \ln \frac{\dot{\gamma}}{c}}\right)_T \qquad (15)$$

The activation energy or enthalpy and activation volume evaluated from the experimental data will generally differ for different deformation mechanisms.

The deformation mechanism is generally different in different temperature regions for a specific metal according to its crystalline structure. There are essentially three major temperature regions for each metal: (a) High temperatures, approximate $0.5T_m < T < T_m$, where T_m designates the melting point temperature. (b) Intermediate temperatures, approximate $0.25T_m <$ T < approximate $0.5T_m$. (c) Low temperatuees, T < approximate $0.25T_m$.

At high temperatures the rate controlling mechanism for BCC metals is most likely the climb of dislocations; at intermediate temperatures the interaction of dislocations with impurities. At low temperatures the problem is more controversial and the suggested rate-controlling mechanisms are nonconservative motion of jogs in screw dislocations, the overcoming of interstitial atoms or precipitates, the cross slip of screw dislocations and the overcoming of the Peierls stress (Conrad, 1964).

III. PREVIOUS INVESTIGATIONS

Pugh (1957) has studied the temperature dependence of the tensile properties of vanadium in the temperature range from 78 to 1300°K but the strain hardening exponent, m, and the strain rate sensitivity, n, have been evaluated only between 500 and 1300°K. A commercially pure calcium-reduced vanadium was used by Clough and Pavlovic (1960) to study the tensile properties and fracture and twinning at temperatures between 77 and 573°K. They found a five-fold increase in yield strength, a threefold increase in tensile strength and a ductile to brittle transition in this temperature range. Both the $\{100\}$ and the $\{110\}$ were identified as active cleavage planes and mechanical twins were formed on $\{112\}$ planes by impact loading at temperatures of 195°K and lower.

Using commercially pure polycrystalline vanadium, Lindley and Smallman (1963) evaluated the effects of grain size and strain rate on the yield stress and flow stress between 20 and 293°K. At and above 77°K, the vanadium deformed solely or predominantly by slip, while at 20°K, deformation was associated with twinning. Single crystals of vanadium have been deformed in compression at 77°K by Edington and Smallman (1965) who found that twin systems were $(\bar{1}21)\ [\bar{1}11]$ and $(211)\ [\bar{1}11]$.

The dislocation configuration and density produced by plastic deformation of vanadium in the temperature range 77 to 673°K have been investigated by Edington and Smallman (1964). In material of constant grain size, the dislocation density N is proportional to the strain ε, and $\sqrt{N}$ is proportional to the flow stress τ over the whole temperature range.

Using available data in previous literature, Conrad and Hayes (1963) have included polycrystalline vanadium in their work on thermally activated deformation of the BCC metals at low temperatures. They found that the activation volume was approximately $50b^3$ when the effective shear stress was approximately 2 kg per sq mm and that this volume decreased to 2 to 5 b^3 at high stresses for all BCC metals.

Christian and Masters (1964), in their extensive studies of low temperature deformation of BCC metals, have generated some data on activation energy and volume for polycrystalline vanadium but stated that difficulties were encountered in deforming vanadium single crystals. Because of the low work hardening and high yield stress, vanadium specimens tended to neck down immediately after yielding at very low temperatures. No data for the change of flow stress with strain rate and temperature have thus been obtained for single crystals at low temperatures. They

also mentioned that a dependence of $(\Delta\sigma)_T$ on purity was found for vanadium, and this still persisted at 90°K , but results for impure vanadium could not be obtained at low temperatures due to brittleness of the material. Consequently, a systematic investigation of $(\Delta\sigma)_T$ for vanadium of two purities has not been made. They used arguments based on the high value of the effective shear stress and its high strain rate sensitivity to conclude that most of the low temperature stress is probably due to a lattice interaction of Peierls-Nabarro force. Furthermore, they stated that it seems improbable that the total impurity level is sufficient to produce the very high stresses at low temperatures. It is of special interest to obtain flow stress measurements on very pure metals in the very low temperature region and these experiments should provide a final answer to this question.

Mitchell, Fields and Smialek (1970) obtained some preliminary results on yield stresses and work hardening characteristics as a function of purity for vanadium single crystals deformed in tension. They used two grades of materials, 99.8% and 99.98% respectively and stresses were resolved onto the (011) <111> system which was the identified slip system for the particular easy glide orientation used in their work.

IV. EXPERIMENTAL PROCEDURES

A. Specimen Preparation

Two grades of high purity vanadium were used in the present work. They are: (a) 99.99% purity produced by Sullivan's (1965) process and supplied by U.S. Bureau of Mines, Boulder City Metallurgical Laboratory, Boulder City, Nevada; (b) 99.93% purity produced by the process developed by Wang et.al. (1970) and supplied by Teledyne Wah Chang Corporation, Albany, Oregon.

The 99.99% purity vanadium received was of dendritic form (Sullivan, 1965) which was then electron beam melted into a 3 in. diameter ingot. After a slight scalping, the ingot was forged and swaged at room temperatures to 1/4 inch diameter rods. This material was partly used for polycrystalline specimens and partly for mono-crystalline specimens. In the former case, the rod was machined into tensile specimens with the gauge dimension of 0.140 in. dia. x 0.500 in length; both ends beyond the gauge were of 0.225 in. dia. x 0.200 in. length respectively. Machined specimens were then annealed in a vacuum furnace at 870°C (1600°F) for one hour for re-crystalization. The average grain size was 30 grains per mm^2.

The 99.99% purity material used for monocrystalline specimens was grown into single crystals with predetermined orientation by electron beam floating zone technique at Oak Ridge National Laboratory, Oak Ridge, Tennessee. (Appendix I), two passes were used in each case. The first pass was ordinarily carried out in a vacuum of 10^{-7} to 10^{-8} torr range while the second pass was in the 10^{-9} to 10^{-10} torr range. By the seeding technique, two particular orientations, i.e., <110> and <112>, of monocrystalline rods, each 0.225 in. diameter by 7 in. length, were obtained. The <110> orientation was chosen because the plastic flow stress is essentially independent of past history. That is to say, the flow stress is essentially constant after yielding in specimens with this orientation (Rose, Ferriss and Wulff, 1962). It was hoped that the differential flow stress due to change of temperature or strain rate would be little affected at different stages of straining. The orientation, <112> axis, with less symmetry in relation to slip systems, was chosen for comparison, expecting that the orientation dependence of flow stress (Rose, Ferriss and Wulff, 1962; Bowen, Christian and Taylor, 1967) could be examined.

The monocrystalline rods were sawed into 7/8 inch. lengths using diamond impregnated copper abrasive

cutting wheel. During sawing, the rod was held in position by solidified resin in order to avoid any macrostrain. To prepare the gauge section, 0.140 in. dia. x 0.500 in. length, an electropolishing apparatus (Fig. 2) was employed. The principle for construction was similar to that of Avery, Ebner and Backofen (1958). A stainless steel wheel, dipped into an aqueous solution of 15% oxalic acid by weight, was used as the cathode. The wheel was driven by a motor rotated at approximately 8 rpm. The specimen, held directly by the chuck of the drill motor, was rotating in the reverse direction at approximately 2 rpm. With a total current of 0.5 amp. running from the specimen to the wheel and then to the bath, the voltage drop between the specimen and the wheel was 2 volts and that between the latter and the bath was 4 volts. A shunt circuit was connected between the power source and the wheel, and there was more current flowing through it than between the specimen and the wheel, so that the possible metal accumulation on the wheel face was eliminated. Because of the continuous film of electrolyte maintained between the specimen and the wheel, the danger of sparking was reduced. The total operating time for completing one specimen was about two hours. The tolerance of the gauge so polished was plus and minus 0.002 in. diameter. At least two back reflection Laue diffraction

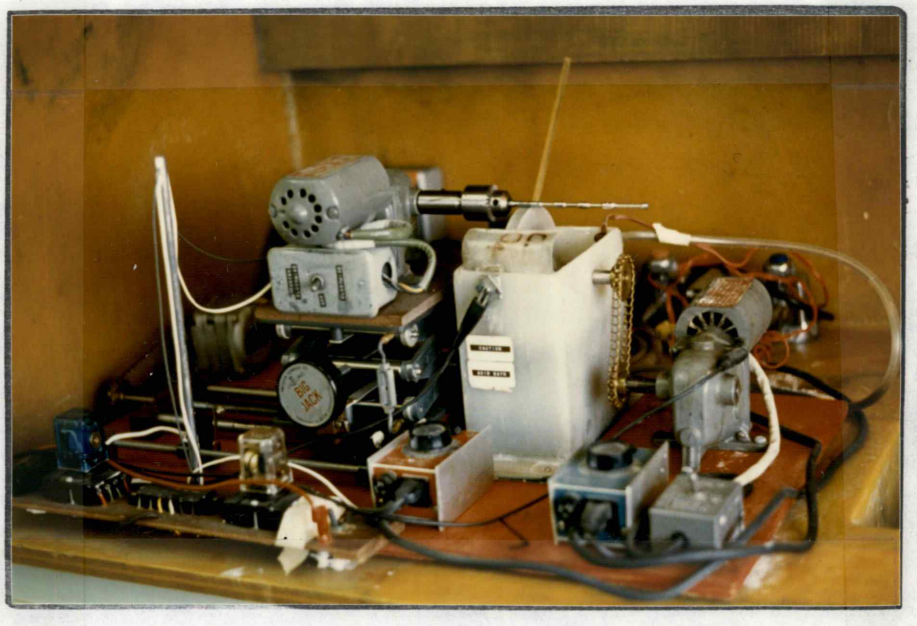

Figure 2

Electropolish Apparatus, including a polyethylene tank, a motor driven stainless steel wheel, another motor for rotating the specimen and a positioning device which can travel vertically and horizontally.

patterns were taken at the gauge section of each specimen in order to evaluate the perfection and orientation of the crystal. The first one was exposed at a marked position with the tensile axis perpendicular to the x-ray beam and the second one was performed after the specimen was rotated 90 degrees from the original position using the tensile axis as rotating axis. The accuracy of orientation of the tensile axis of the specimens, both for <110> and <112> crystals, was well within 2 degrees. No imperfection or distortion was noticed except that a portion of the <110> rod, designated C, which was reported to have fluctuation of power during zoning, showed distinctive subgrain boundaries with approximately 2 degrees of misorientation. These specimens were rejected for tensile testing. The back reflection photographs of perfect and imperfect crystals are shown in Fig. 3; the photomicrographs of a normal single crystal are shown in Fig. 4. It is apparent in the latter figure, that dislocations are lined up to form a small-angle subgrain-boundary.

In order to improve the surface finish of monocrystalline specimens, they were then polished in a Buehler 1721-2 electropolishing cell. The specimen was surrounded by a cylindrical stainless steel cathode, immersed in aqueous electrolyte containing 10% sulfuric acid. The electrolyte was constantly agitated during polishing and the voltage and current maintained at 2 volts and 0.2 amperes

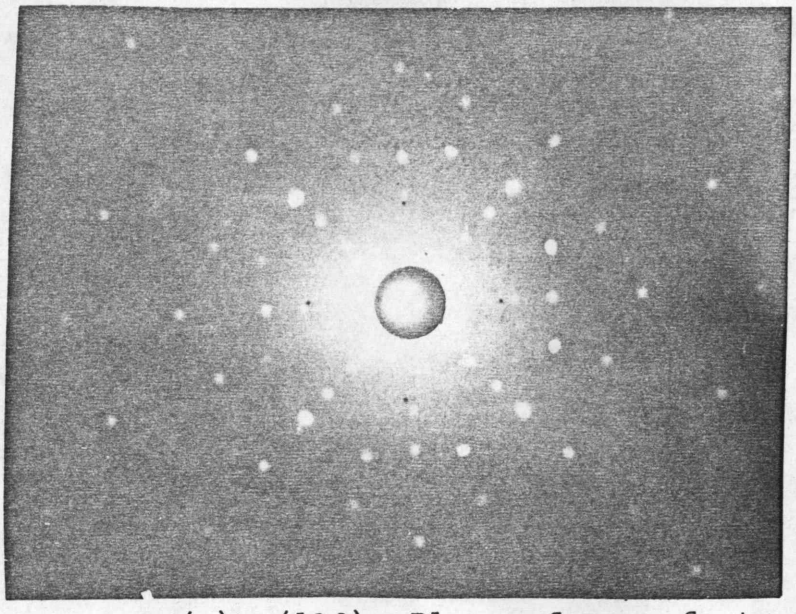

(a) (100) Plane of a perfect crystal with <110> axis

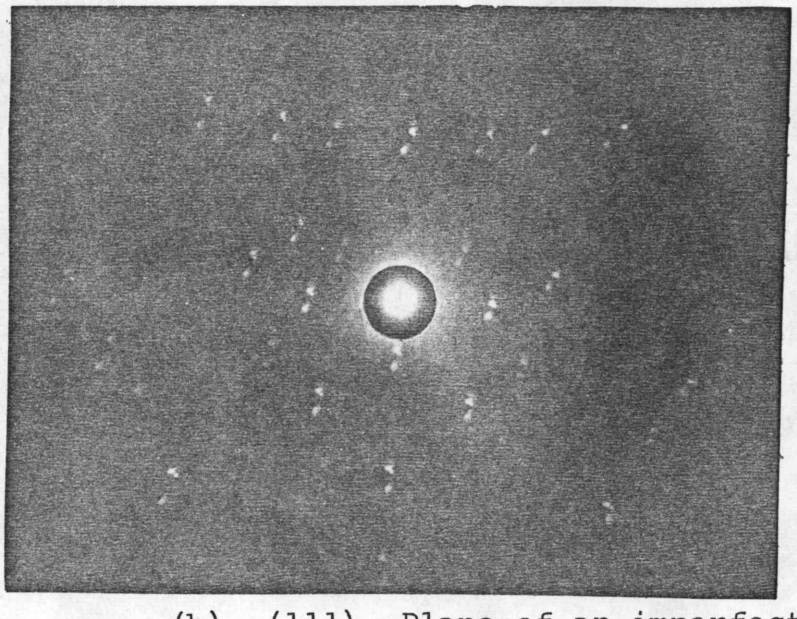

(b) (111) Plane of an imperfect crystal with <110> axis

Figure 3: Back reflection laue pattern of vanadium single crystals.

(a) 150X

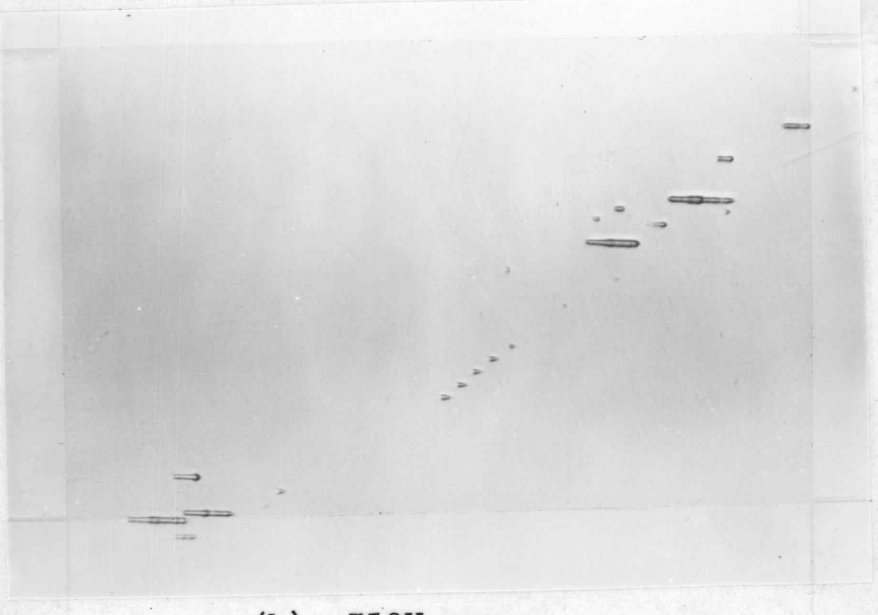

(b) 750X

Figure 4: Photomicrographs of a 99.99% vanadium single crystal showing subgrain boundaries formed by dislocations.

respectively. The time for this final polishing was approximately 10 seconds.

The 99.93% purity vanadium received was of rod form with a diameter of 1/4 in. which was previously forged, rod rolled and then swaged from a 9 in. diameter electron beam melted ingot. The rods were machined into tensile specimens the same as that mentioned for 99.99% purity polycrystalline specimens. They were then annealed in a vacuum furnace at 1090°C (2000°F) for one hour for full recrystalization. The average grain size obtained was 100 grains per mm^2.

Chemical data for the materials used in the present work are compared with those used for previous deformation investigations in Table 2. It is to be noted that high purity vanadium is sensitive to interstitial pick-up during handling, e.g., electron beam melting or vacuum annealing under ordinary vacuum atmosphere, 10^{-4} torr. The nominal 99.99% polycrstalline material was actually at the level of 99.98%. Single crystals were of the highest purity among all materials used in the present work. Analyses applied only to the starting material such as 99.98% vanadium indicated by Mitchell, Fields and Smialek (1970) might be misleading.

These authors used two grades of vanadium and studied the resolved yield stress as a function of temperature from 77°K to 400°K. Typical shear stress-

TABLE 2

Chemical and Hardness Data of Vanadium Used in The Present and Previous Investigations

Reference	Purity %	Form	Hardness DPH	Impurities ppm(6) C	H	N	O
Present	99.99	Dendrites(1)		12	43	2	18
	99.99	P.C.(2)	54	43	3	80	130
	99.99	S.C.(3)	43	7	8	35	59
	99.93	P.C.(4)	60	150	3	73	183
Pugh(1957)		P.C.		900	4	700	570
Clough and Pavlovic(1960)		P.C.		360	40	830	700
Lindley and Smallman (1963)		S.C.		170	<5	80	1700
Conrad and Hayes(1963)		P.C.		470	43	520	700
Christian and Masters (1964)		P.C.(5)	115	(Not Indicated)			120
Edington and Smallman(1965)		S.C.		100		700	300
Greimer and Boulin(1967)		S.C.		300		200	300
Mitchell,Fields, and Smialek (1970)	99.98	S.C.		20	<10	<10	70
	99.8	S.C.		250	<5	184	368

Remarks: (1) Dendrites: Electrorefined before consolidation. Other impurites analyzed are: Al, 7ppm: Cu,<5; Mg,2; Mn,4: Ni,<4; Si,15.
(2) 99.99% P.C.: Polycrystals.
(3) 99.99% S.C.: Single Crystals
(4) 99.93% P.C.: Polycrystals. Other major impurites: Al,92ppm; Si,188; Mg,35; Fe,<50.
(5) Other major impurities: Al,60ppm; Fe,500; Si,200; Y,1000.
(6) ppm: parts per million by weight

shear strain curves at temperatures between 273 and 500°K for vanadium single crystals were also investigated. Materials used for deformation tests by other investigators all contained significant amounts of impurities. Christian and Masters (1964) in their extensive work on BCC metals including polycrystalline vanadium, did not indicate the exact chemical analyses of carbon, hydrogen nor nitrogen but mentioned that the microhardness was 115 DPH. According to the correlation between the hardness and interstitial elements demonstrated by Bradford and Carlson (1962) and Thompson and Carlson (1965), the total interstitials should have been somewhere between 500 and 1000 ppm. However, with addition of 1000 ppm of yttrium, (Table 2), an effective gettering agent, the behavior of deformation of this material should be similar to the 99.93% purity polycrystals used in the present work. Because of the grain refining effect of yttrium, the grain size of their polycrystalline specimens was 5000 grains per mm^2, although this was partly attributed to a lower temperature, 1000°C, employed for recrystalization annealing. Their data will be used for comparison in later sections.

(B) Tensile Testing Procedures

The machined or electropolished specimen was held by a split-type holder which, in turn, was threaded in

a cap-nut. Some single crystal specimens and the holder set, which is made of stainless steel, are shown in Fig. 5. The holder set was connected with a 1/4 in. diameter pin to a grip bar which, in turn, was mounted on a floor model TT Instron Tensile Machine through a ball joint. A stainless steel coolant container, 4 in. diameter x 1/16 in. wall x 6 in. tall, was welded on the lower grip bar so that the specimen and the holder set would be well immersed in the coolant while it was filled in the container. For intermediate temperature tests, when liquid nitrogen and other liquid coolants were used, three small cups, 1 in dia, x 1/16 in. wall x 7 in. tall, were placed inside the container. The coolant container-and-cup set mounted on the Instron Machine are shown in Fig. 6. The whole coolant container set was encased inside a Styroform case packed with glass wool between the former and the latter so that the Styroform case would be held in position by friction. The lid of the Styroform case consisted of two halves, so that they could be removed from the top of the case during filling.

There were holes at the bottom of the case for the lower grip rod and drainage hoses to pass through.

Six temperatures were used for testing as follows: (a) 77°K, liquid nitrogen boiling point; (b) 120°K,

(a) Some single crystal tensile specimens and grips

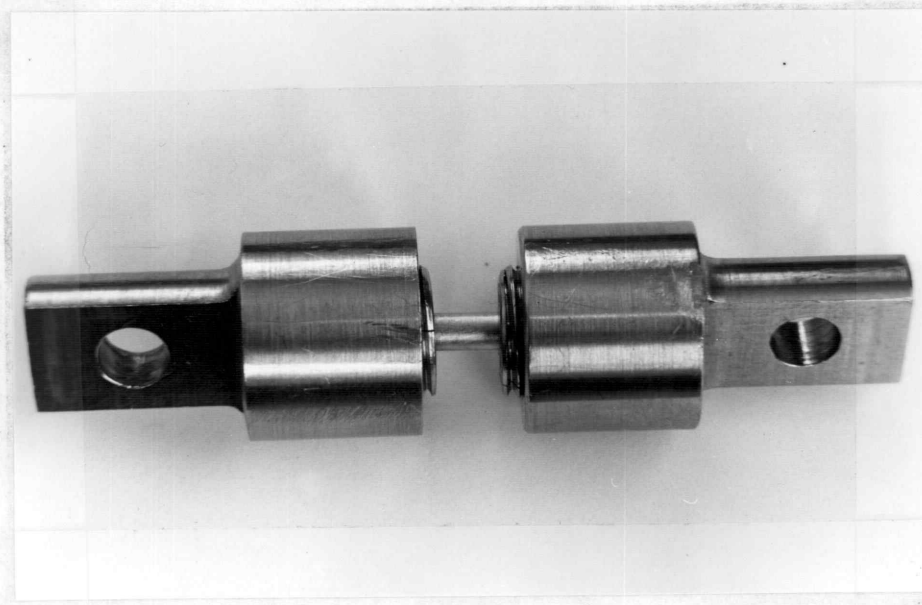

(b) Tensile specimen held by grips

Figure 5. Vanadium single crystal tensile specimen and grips.

Figure 6

Tensile grips and coolant container set mounted on the Instron Machine.

freezing point of isopentane; (c) 160°K, freezing point of methyl alcohol; (d) 200°K, constant temperature liquid methyl alcohol cooled by liquid nitrogen; (3) 233°K, same as above; (f) 293°K, constant temperature water in essential equilibrium with the atmosphere in the laboratory which was air conditioned and maintained at 293°K.

A copper vs constantan thermocouple in contact with the gauge section of the specimen was connected to a potentiometer to measure the testing temperature. The liquid coolant was constantly stirred and the exact temperature was equilibrated for approximately 10 min. before testing. The variation of temperature during tests was within plus and minus 2°K.

Some polycrystalline material was machined into specimens with a 1 in. reduced section, on which knife edges positioned 1/2 in. apart were clamped and connected with an extensometer to evaluate the Youngs Modulus at 293°K and 77°K

Other tests for determination of slip planes and twinning planes were performed at constant temperature and constant strain rates for a total plastic strain of a few percent. The crystallographic aspects of the slip and twinning planes were determined from the orientation of traces of the planes on the crystal surface.

The technique was the same as that described by Barrett (1966) and illustrated by Schadler (1960).

Since both the slip direction and the shear displacement for twinning have been well established for BCC metals to be <111> (Honeycombe, 1968), no attempts were made to determine the slip direction.

Two major types of experiment were carried out: temperature change and strain-rate change. For the temperature change experiments, 293°K was used as a reference temperature and the specimen was deformed alternately at 293°K and a second temperature. During the temperature change the load was relaxed to about 80% of the higher temperature flow stress in order to prevent recovery due to the strain annealing effect. The time for changing from one temperature to a second one ranged from 15 minutes to 1 hour, depending upon coolant manipulation problems. The strain rate was maintained constant at approximately 6.67×10^{-5} sec. $^{-1}$. In order to prevent necking down immediately after yielding and to decrease the probability for twinning at low temperatures, the specimen was prestrained at

293°K to about 4% elongation before changing to a lower temperature (Christian and Masters, 1964). Then the temperature was changed after each 2% elongation until a total elongation of about 20% was reached. Straining beyond this point usually resulted in necking down and no homogeneous deformation could be obtained.

For the strain-rate change experiments, specimens were prestrained at 293°K to about 2% of elongation for the same reason as mentioned above for the temperature change tests. The temperature was then changed to the desired value and the specimen deformed at a strain rate of approximate 6.67×10^{-5} sec.$^{-1}$; the strain rate was changed to 6.67×10^{-4} sec.$^{-1}$, by simply flipping the switch on the Instron Machine after each additional elongation at the temperature. It should be noted that the strain rate mentioned in the present paper is actually a calculated value based on the displacement of the cross head of the tensile machine and the gauge length of the specimen. When the moving speed of the cross head changed from a low value to a high one, which is 10 times greater, while the moving speed of the recording chart maintained the same, the magnification of the elongation on the chart was then 10 times smaller. In order to have a readable

curve on the chart, approximately 2% elongation of strain was necessary at the higher strain rate, but, only about 0.2% elongation of strain was needed at the lower strain rate. Therefore, the tests were performed at the higher strain rate for 2% elongation and, then, at the lower rate for 0.2% elongation. The changing of strain rate was repeated until a total elongation of about 20% was reached.

V. EXPERIMENTAL RESULTS

(A) DETERMINATION OF YOUNGS MODULUS, SLIP AND TWINNING PLANES.

As mentioned above, some polycrystalline specimens with a reduced section of 1 inch were used for Youngs Modulus determinations. Knife edges positioned 1/2 in. apart were clamped on the gauge section of the specimen and connected to a microformer type of extensometer. The latter, in turn, was connected with the chart driven system of the Instron Machine so that the load-elongation curve was directly recorded on the chart. By measuring the slope of the initial line portion of the curve, the Youngs Modulus for the polycrystalline material was obtained. Experiments were performed both at 77°K and 293°K and the results were 1.30×10^4 kg/mm^2 in both cases. This agrees fairly well with the data in the literature (Foote Mineral Co, 1968).

Youngs Moduli for single crystals of <110> and <211> tensile axes, hereafter referred to as <110> and <211> crystals, were calculated from the elastic constants determined by Bolef (1961) and they were 1.26×10^4 and 1.27×10^4 kg/mm^2 respectively. (see Appendix II).

For all other tensile tests, no extensometer was used and the recorded strain on the chart was actually the displacement of the cross head of the tensile

machine. The displacement was the sum of the elongation of the specimen and the strain of the parts of the machine. The latter should be eliminated in order to obtain the actual strain of the specimen. The Youngs Moduli were used to calculate the initial strain at the proportional limit and, therefore, the actual strain was obtained (Appendix III). The maximum shear stresses of polycrystalline specimens were obtained by multiplying the axial normal stresses by 0.5 (Harding, 1969).

Among those experiments for slip plane determination, two <110> crystals deformed at 77°K showed a ductile chisel edge type of fracture (Fig. 7), which was observed by other investigators in BCC metals (Rose, Ferriss and Wulff, 1962). By using the back reflection Laue X-ray technique, it was found that the knife edge was in the <110> direction. Other <110> crystals showed the same tendency to neck down, i.e., to reduce symmetrically in one dimension but remain the same width as it was before deformation in the other dimension. Atkinson et al. (1954) found the same results in tungsten when deformed at high temperatures and claimed that this was due to four active $\{110\}$ <111> slip systems operating at roughly equal rates. However, the resolved shear stress on the $\{211\}$ planes is higher than that on the $\{110\}$ planes, by a ratio of 1.16 to 1. It is believed

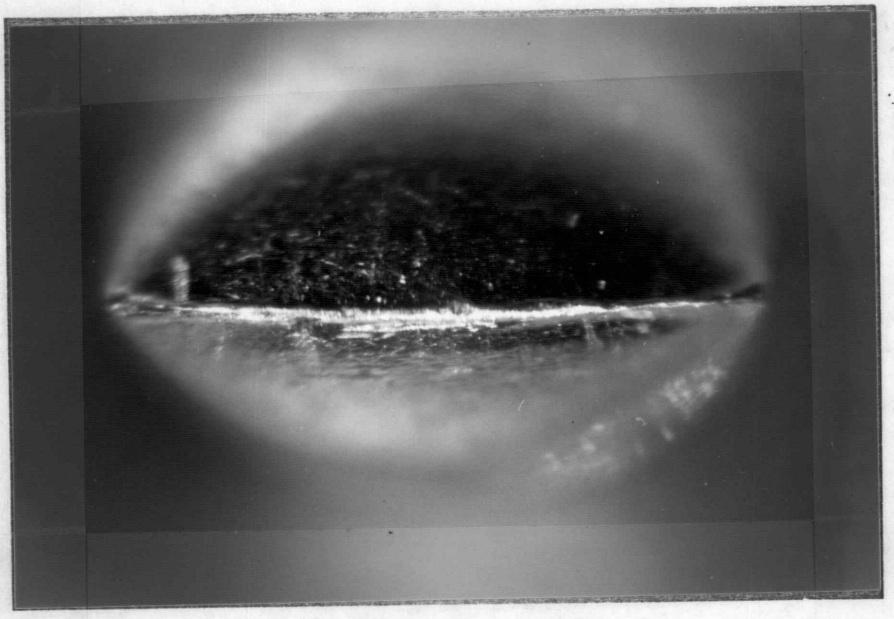

(a) Top view, 30x

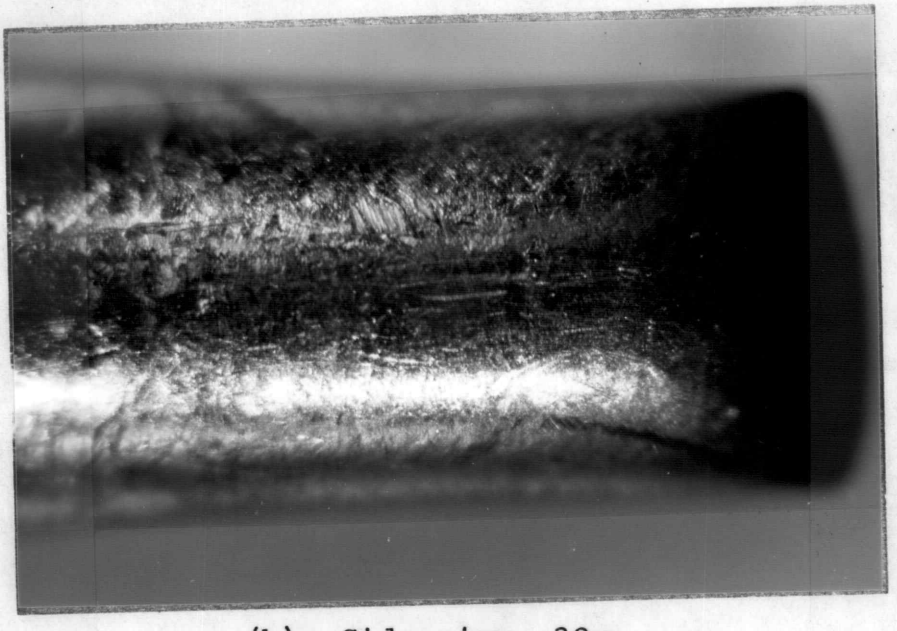

(b) Side view, 30x

Figure 7: Typical chisel edge fracture of crystal C-1, deformed at 77°K. Initial axis of specimen was <110>.

that the chisel phenomenon was caused by a double slip simultaneously on $(112)\ [11\bar{1}]$ and $(11\bar{2})\ [111]$ systems. The resultant slip direction for these two is $[110]$.

In general, no distinct slip lines were observed for these tests except for <110> crystal F-4, which showed some brittle fracture, when deformed at 160°K. Slip lines on the surface viewed from (001) and $(\bar{1}10)$ disrections are shown in Fig. 8. Two sets of straight slip lines symmetrical to the tensile axis are apparent when viewed from the $(\bar{1}10)$ direction, while a wavy texture and cross slipping can be observed in the view in the (001) direction. The predominant slip planes were determined to be the $\{112\}$ and the active slip systems $(112)\ [11\bar{1}]$ and $(11\bar{2})\ [111]$, which are conjugate to each other.

Electron photomicrographs of the same crystal viewed from two different directions are shown in Fig. 9. The fineness of the slip lines are revealed in these highly magnified views, The tensile specimen F-4, was then cold mounted in Areolite, ground, polished and viewed microscopically. No trace of lines were noticed. This indicates that these lines were slip lines rather than twins. Because no misfit of atoms will occur between either side of the slip plane after slipping, no traces should be left underneath the surface.

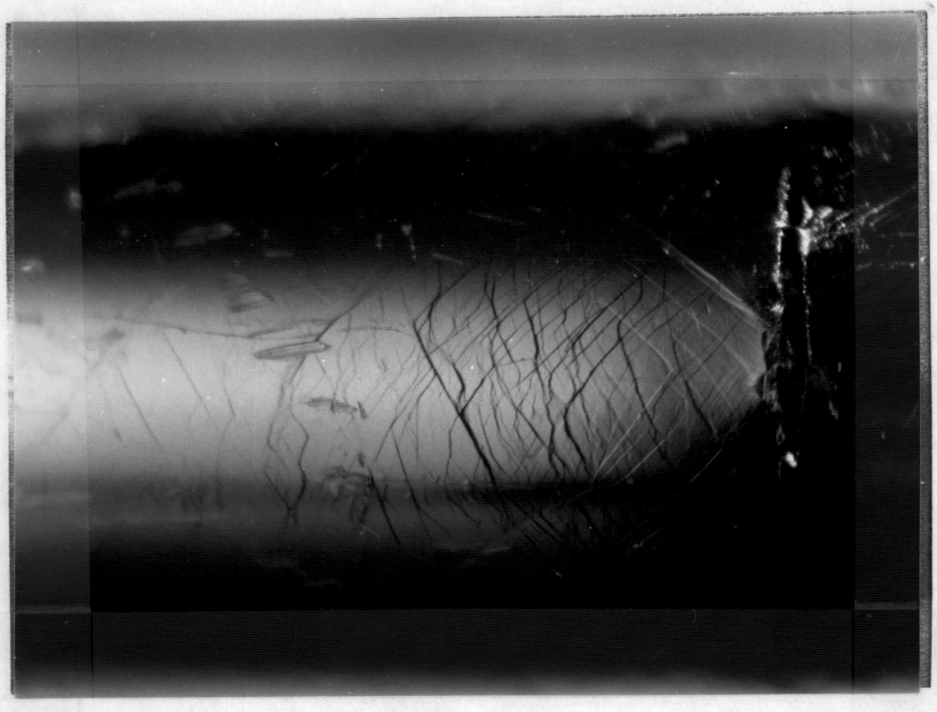

(a) View in <001> direction, 30X

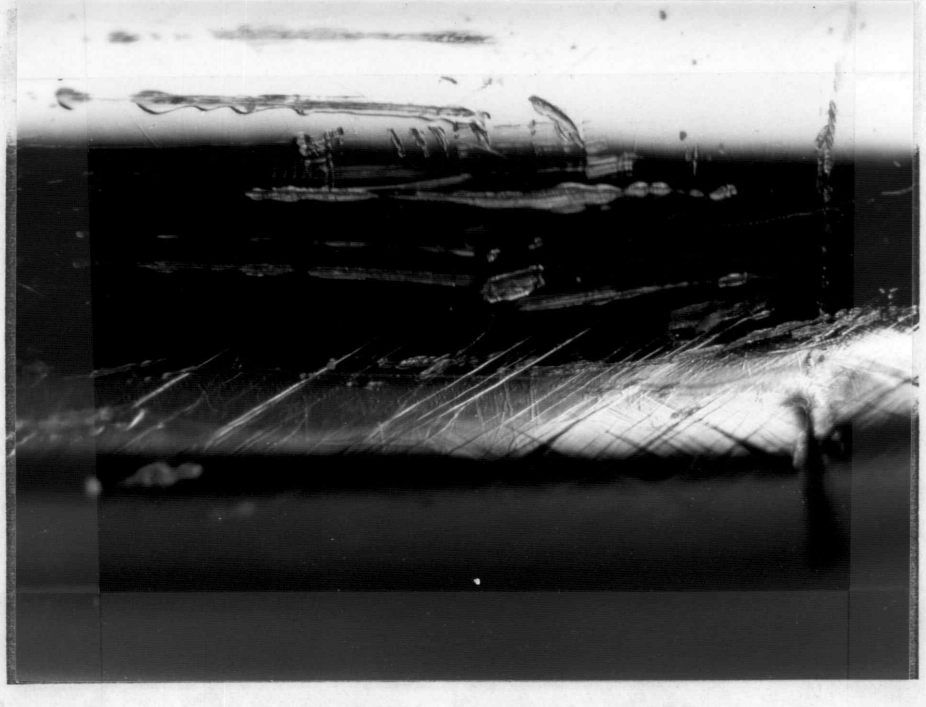

(b) View in <110> direction, 30x

Figure 8: Single crystal F-4, deformed at 160°K. Initial axis of specimen was <110>.

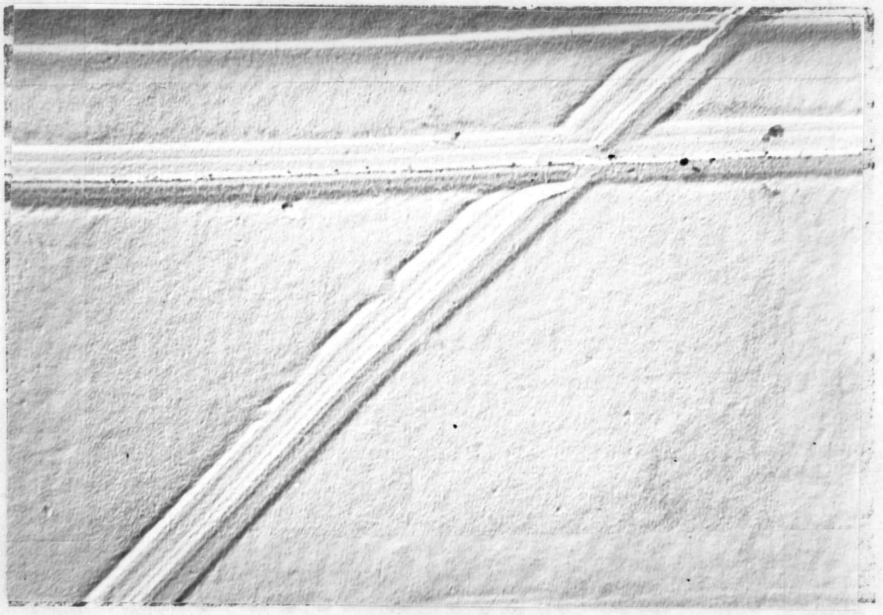

(a) View in <100> direction, 21,000X

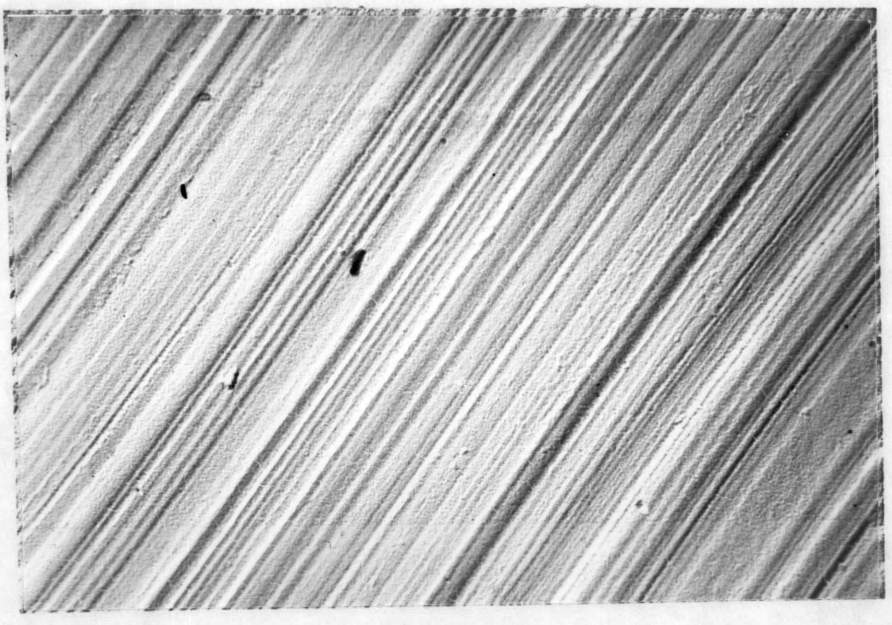

(b) View in <110> direction, 21,000X

Figure 9: Electron Microscopic View of Single Crystal F-4, double replica. Axis of specimen was <110>.

The crystal, F-3, next to and sawed from the same rod as F-4, also showed brittle fracture during deformation. The former was then analyzed and the results were: C,15ppm; N,52ppm; 0,76 ppm; and H, 10 ppm. This was higher than the average interstitial content of 99.99% single crystals (Table 2), and probably was the cause of the brittle fracture.

Two <211> crystals deformed at 77°K demonstrated a serrated stress-strain curve accompanied by a clicking sound which is typical of twinning. The specimen was examined after deformation and twins were apparent to the naked eye as well as microscopically. Fig. 10 shows two views of the gauge section of the specimen with heavy markings of twins.

There was a somewhat similar chisel edge at the necked section of the <211> specimen as that for the <110> crystal mentioned above. However, it is apparent from the photographs that the reduction occurred in both transverse directions of the tensile specimen, although the reduction in one dimension was much greater than that in the other dimension. This is expected because the necking down is caused by slipping. If the active slip systems for a $(\bar{2}11)$ crystal were $(121)\ [1\bar{1}1]$ and $(112)\ [11\bar{1}]$, then the slip directions have components in both of the transverse directions of the specimen and a reduction in both dimensions would be obtained which

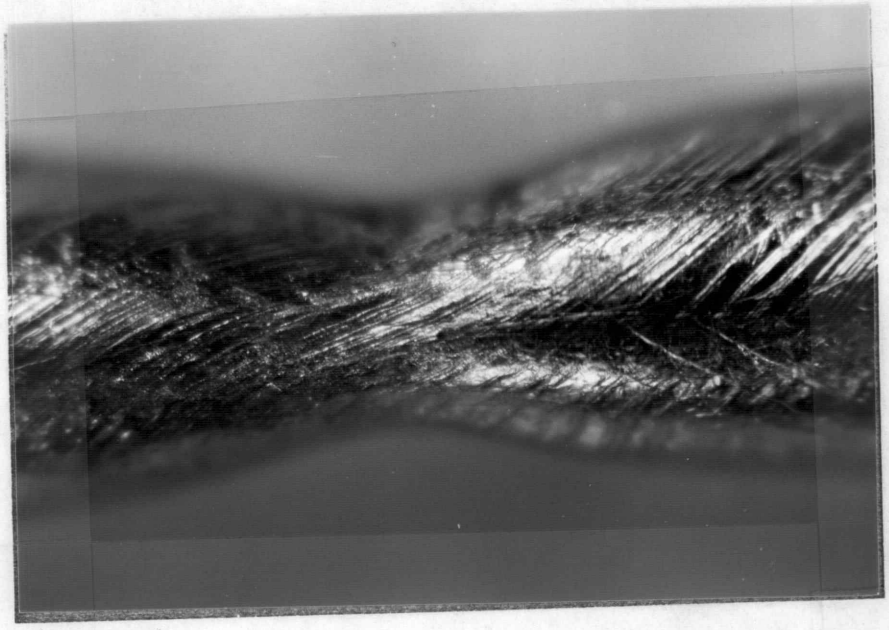

(a) View at one end of the chisel edge.

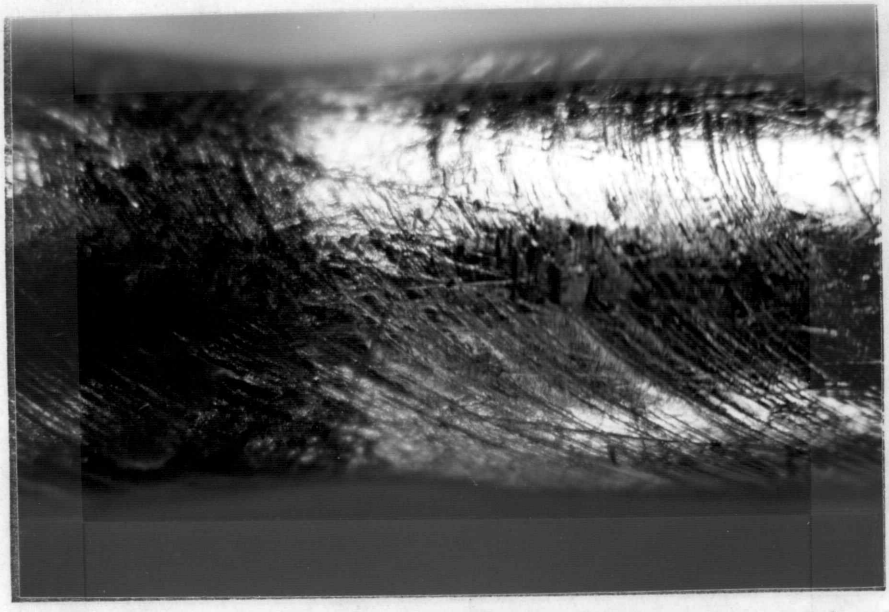

(b) View at 90° from the developing chisel edge, showing slight necking in this dimension.

Figure 10: E-6 crystal with <211> axis deformed at 77°K Heavy markings are twins.

agrees with the observation.

The twinning planes determined from the markings of a <211> crystal were found to be {211}. The deformed <211> crystal was then cold mounted in Areolite, ground, polished and viewed microscopically. The markings could also be detected in the polished specimen which confirms their identification as twin boundaries. (Fig. 11)

(B) Yield, Necking, Twinning, and Fracture Phenomena

All polycrystalline specimens deformed at room temperature (Fig. 12) showed sharp yield points or yield drops followed by a short section of yield elongation and then gradual work hardening. However, single crystals of two orientations, which yielded at very low stresses, showed a very smooth transition from elastic to plastic deformation.

Comparing <110> with <211> crystals, the latter had lower yield stress and an even lower work hardening coefficient at room temperature. It is also interesting to point out that at this temperature the yield stress of the 99.93% polycrystalline specimen was about double that of the 99.99% specimen.

Only a few specimens were used for straining at low temperatures without prestraining at ambient temperature and they are shown in Fig. 13. Again 99.99% and 99.93% polycrystals showed slight yield drops at

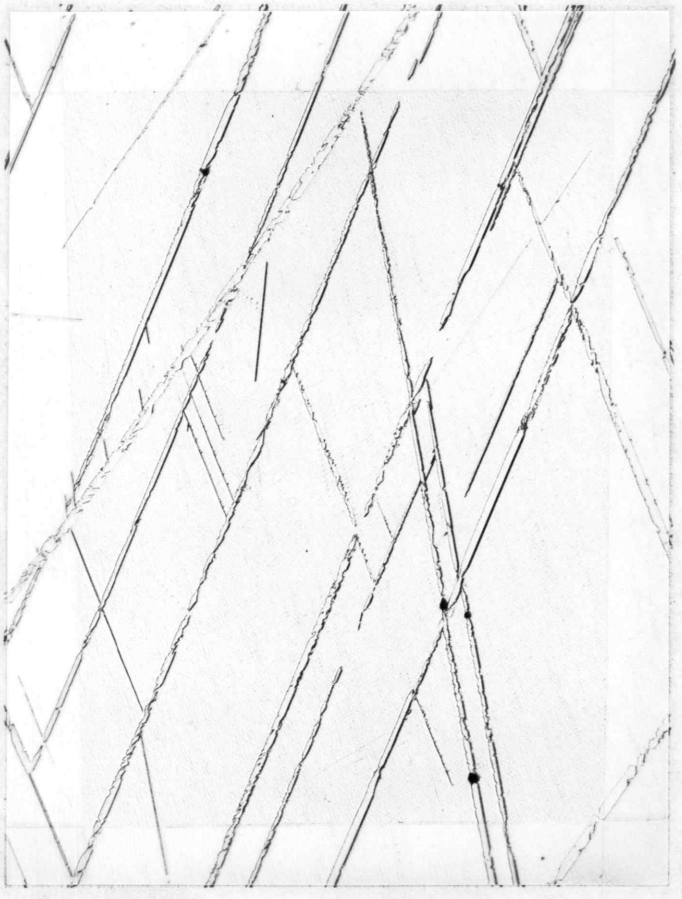

Figure 11

Longitudinal cross section view of crystal E-6, deformed at 77°K, cold mounted, polished and etched, showing distinct twin markings. Initial axis of specimen was <211>

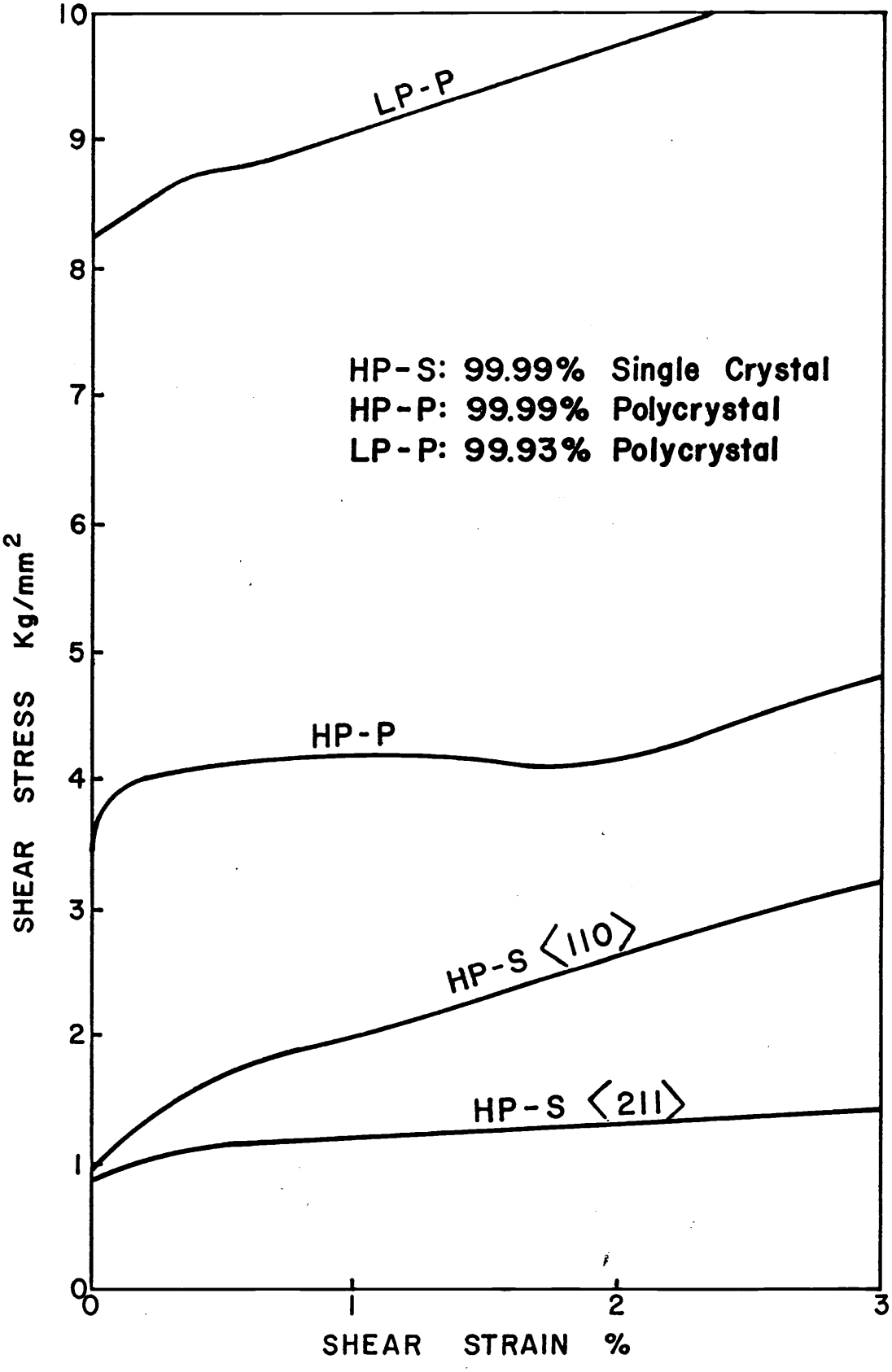

Fig. 12 Typical Room Temperature Yield Curves of Vanadium <110> or< 211> designates tensile axis of specimen.

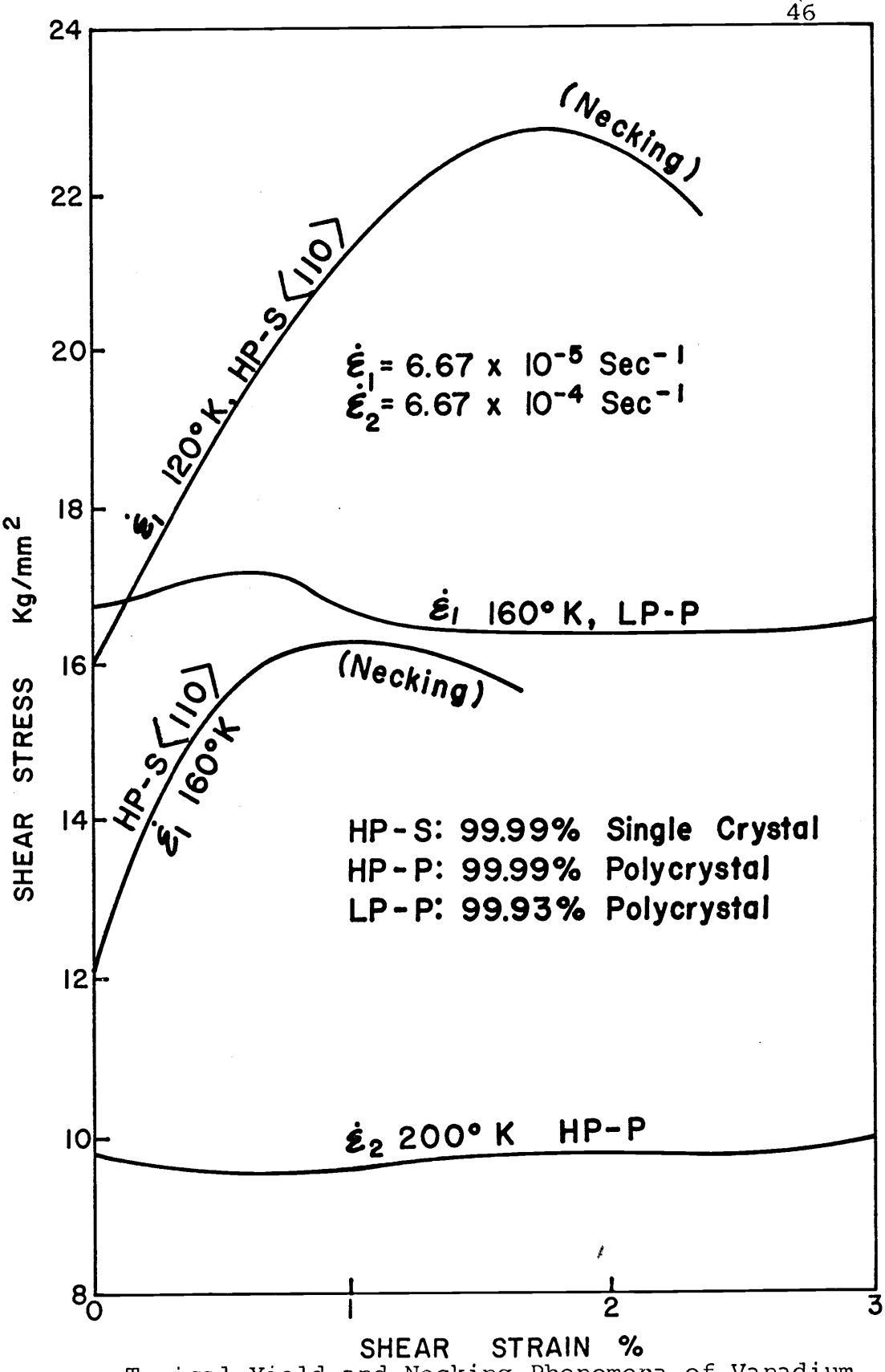

Fig. 13 Typical Yield and Necking Phenomena of Vanadium. ⟨110⟩ designates tensile axis of specimen.

200°K and 160°K respectively; both were successfully strained without quick necking down or fracturing. On the other hand, 99.99% <110> single crystals necked just beyond the yield point both at 160°K and 120°K.

In order to compare the results based on the same procedure and to avoid a quick necking down, all experiments for temperature change and strain rate change were performed at low temperatures after prestraining at ambient temperature.

Single crystals twinned readily at 77°K even after prestraining at ambient temperature (Fig. 14).

Most single crystals gave ductile fractures, e.g., chisel edges as mentioned in the previous section, at temperatures ranging from 293°K to 77°, except that 3 or 4 specimens showed some brittle fracture which was probably due to interstitials picked up during handling, as mentioned above.

(C) Temperature Change and Strain Rate Change Curves.

The typical shear stress versus shear strain curves are shown in Figs. 14, 15 and 16. The shear strain for polycrystals was obtained by multiplying the axial strain by 2. At 293°K, the flow stress of the 99.93% polycrystal was about double that of the 99.99% polycrystal, but at 77°K the flow stresses of both materials

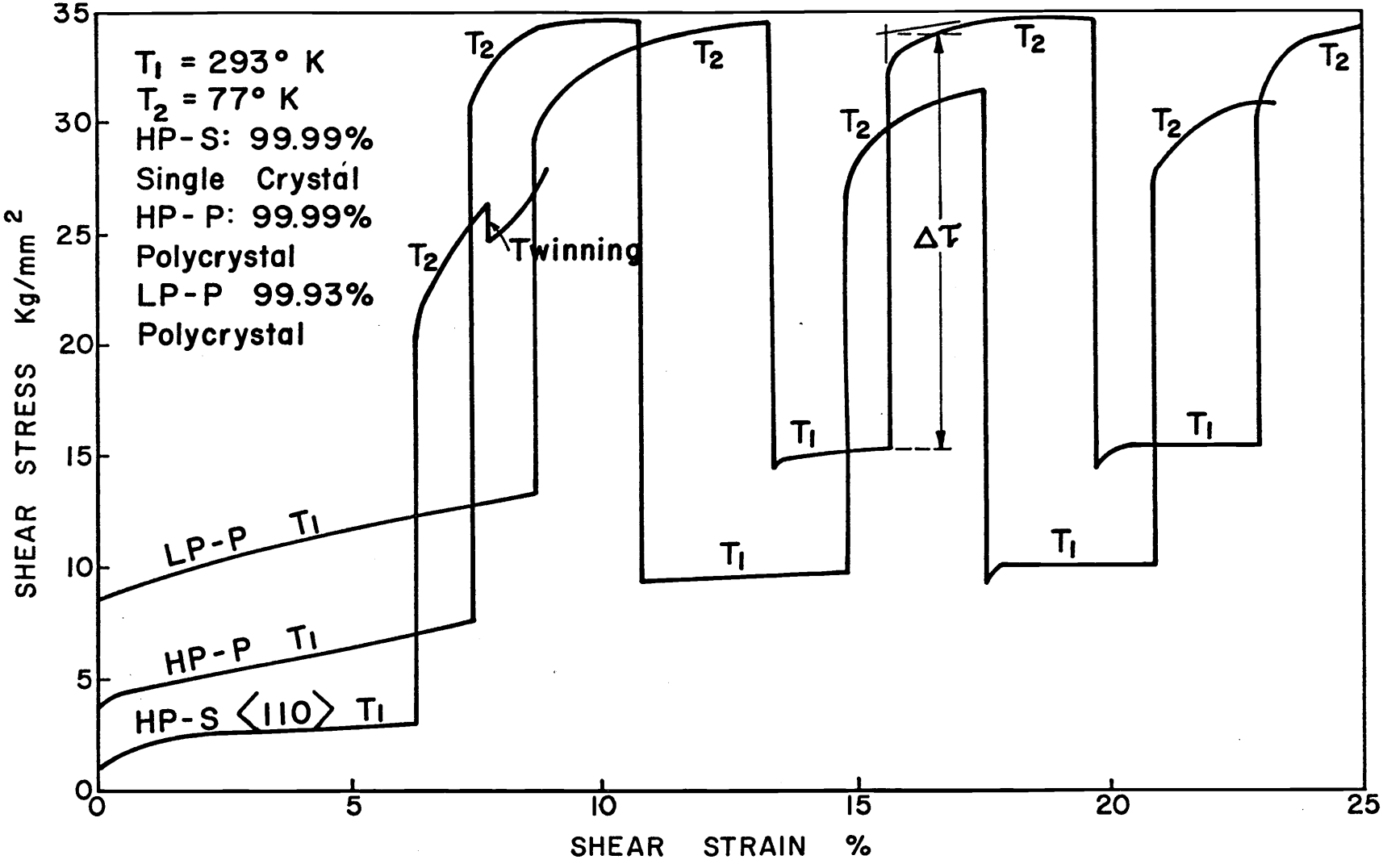

Fig. 14 Typical Temperature Change Curves of Vanadium Between 293°K and 77°K. ⟨110⟩ designates tensile axis of specimen.

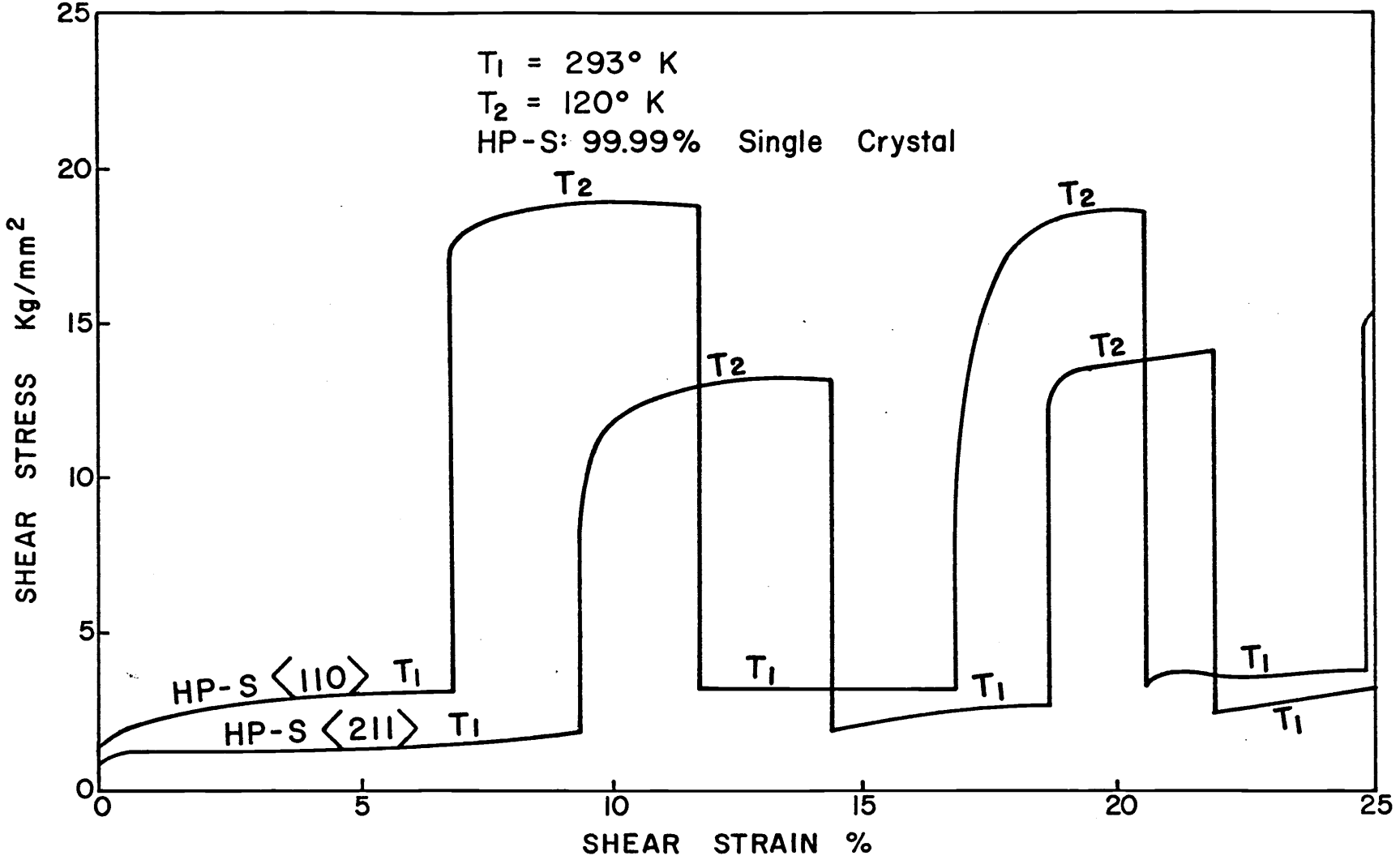

Fig. 15 Typical Temperature Change Curves of Vanadium Between 293°K and 120°K. <110>or <211> designates tensile axis of specimen.

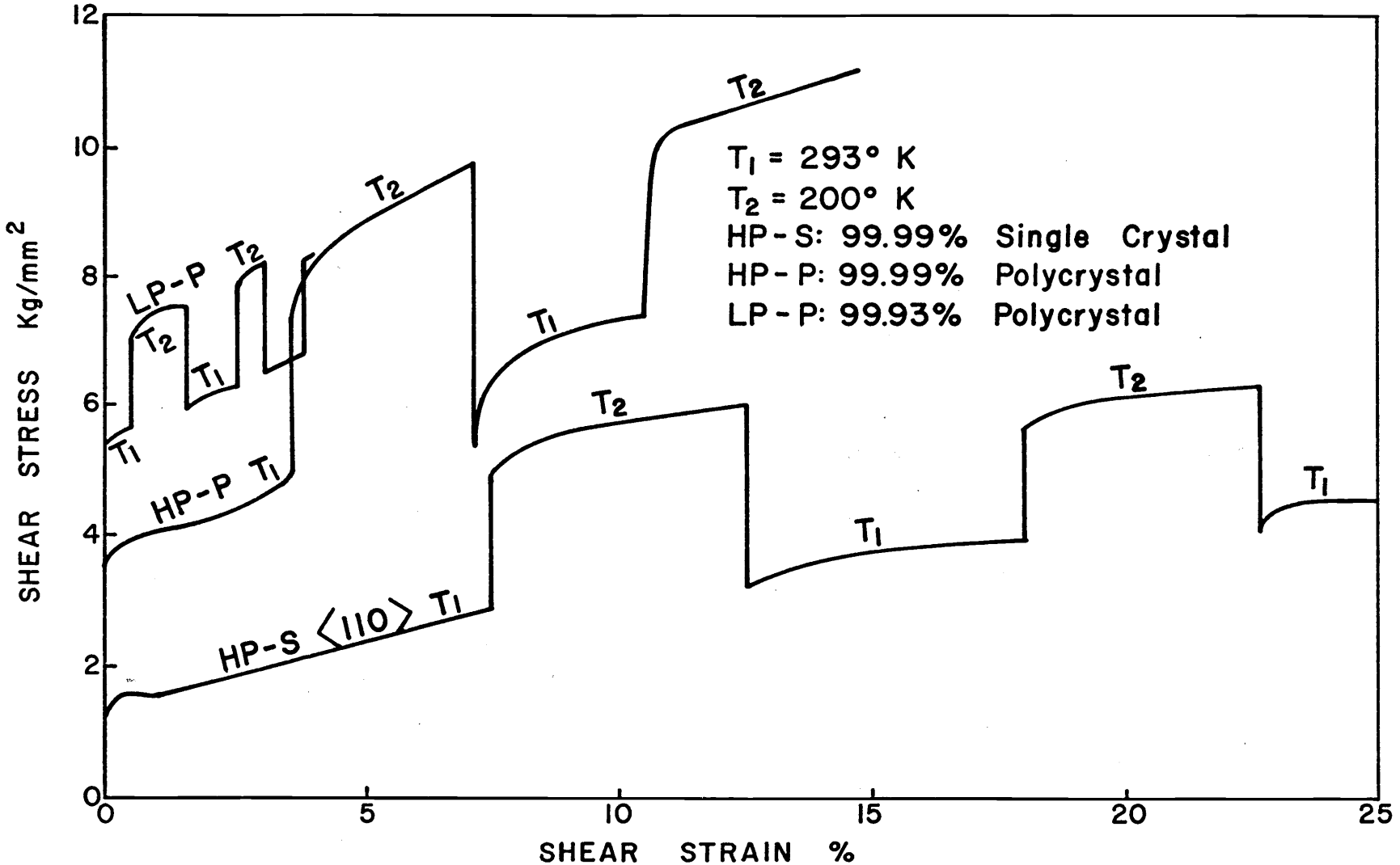

Fig. 16 Typical Temperature Change Curves of Vanadium between 293°K and 200°K. ⟨110⟩ designates tensile axis of specimen.

were about the same. Therefore, the differential stress due to temperature change between 293, and 77°K, was greater for the 99.99% than for the 99.93% specimens. The method of evaluation of the stress change was obtained by extrapolating linearly to the same strain as illustrated in Fig. 14. This should give the flow stresses at different temperatures corresponding to the same dislocation configuration, assuming unloading effects to be negligible. The change in flow stress was always measured for a decrement in temperature to avoid possible annealing effects which are apparent in some curves when the temperature is increased.

Except at the first few percent of straining, $\Delta\tau$ was almost constant, i.e., independent of strain. The value in the neighborhood of 16% shear strain was used for later plotting and evaluation. 99.99% single crystals tended to twin at 77°, even when prestrained at 293°,; no data was obtained for these specimens. However, comparing the section of the curve before twinning for the 99.99% <110> crystal to that of the 99.99% polycrystal, it is fair to say that $\Delta\tau$ for both materials was probably of the same magnitude. The data points for both materials coincided in some cases as will be mentioned later in this paper.

Referring to Fig. 15, the resolved yield and flow stresses for the <211> crystal at 120 and 293°K lower than that of the <110> crystal at the same temperatures; $\Delta\tau$ for the <211> crystal was also lower than that of the <110> crystal.

At 200°, (Fig. 16), the flow stress of the 99.93% polycrystal specimen was approximately the same as that of the 99.99% polycrystal, but at 293°K the flow stress of the former was much greater than that of the latter. Hence, $\Delta\tau$ between these two temperatures, of the former was much smaller than that of the latter. The $\Delta\tau$ for the 99.99% <110> crystal was approximately the same as that for the 99.99% polycrystal for temperature tests between these two temperatures.

Fig. 17 shows two polycrystalline strain rate change curves at 77°K and two monocrystalline curves at 120°K. Because the deformation was performed at the lower strain rate, $\dot{\varepsilon}_1$ approximately 0.2% and changed to the higher strain rate $\dot{\varepsilon}_2$ approximately 2% as mentioned above, the flat portion of the original load-elongation curve at $\dot{\varepsilon}_1$ is not obvious after it is replotted into a shear stress-strain curve. The differential shear stress due to strain rate change is almost independent of strain for all curves. The value of $\Delta\tau$ was obtained by extrapolating to the same strain at two different strain rates and only the value for an increment in strain

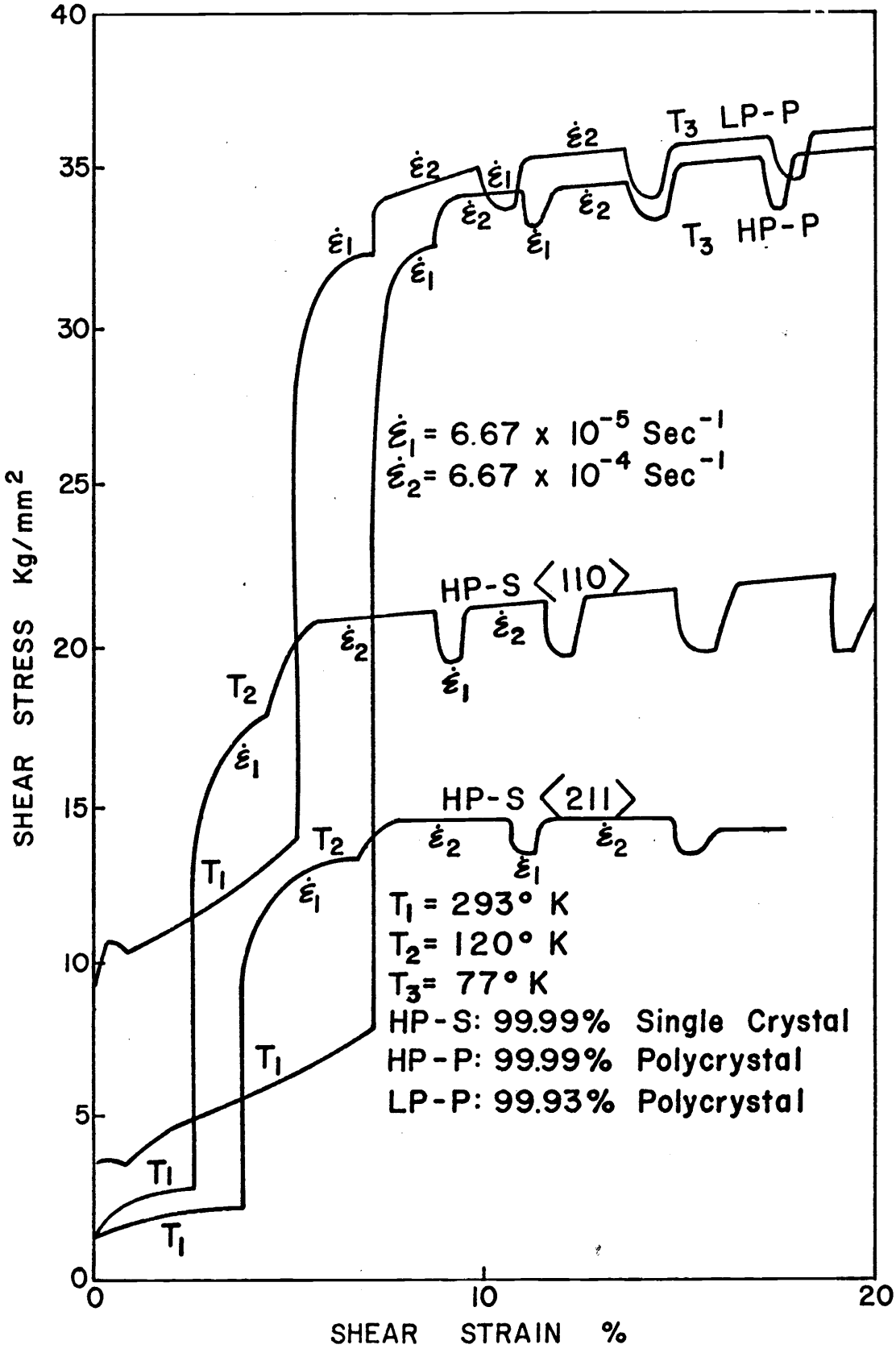

Fig. 17 Typical Strain Rate Change Curves of Vanadium. ⟨110⟩ or ⟨211⟩ designates tensile axis of specimen.

rate was used. It is interesting to note that $\Delta\tau$ due to strain rate change at 120°K gave the largest value among the four curves.

(D) Temperature Dependence of the Resolved Yield Stress, Flow Stress, Activation Enthalpy and Activation Volume.

With the exception of a few early specimens strained directly at sub-ambient temperatures all specimens were prestrained at 293°K and then additionally strained at specific temperatures. The resolved yield stresses were taken at the 0.2% offset from the section of the curve strained at a certain temperature after the mentioned prestraining (Appendix IV).

The resolved yield stress versus temperature curves are shown in Fig. 18 and the effective flow stress, defined as $\tau_T - \tau_{293}$ versus temperature plots are shown in Fig. 19.

For all materials the yield and flow stresses are sharply increased just below 200°K and this is more remarkable for the higher purity than the lower purity. The difference between the stresses for <110> and that for <211> crystals is probably due to the fact the flow stress is dependent on the orientation of the crystal. Rose, Ferriss and Wulff (1962) found the same results in a single crystal of tungsten. The possibility

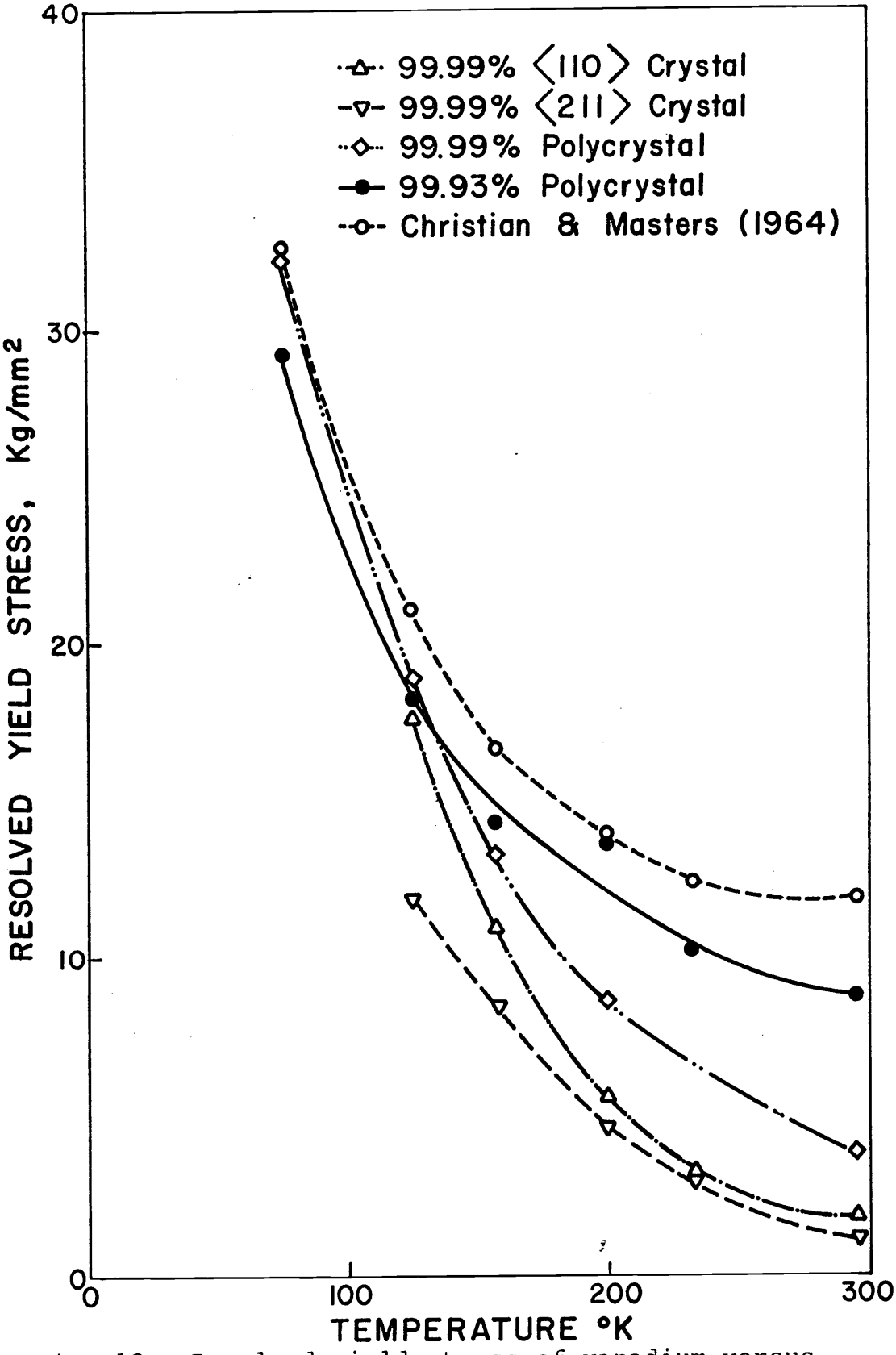

Fig. 18: Resolved yield stress of vanadium versus temperature. ⟨110⟩ or ⟨211⟩ designates tensile axis of specimen.

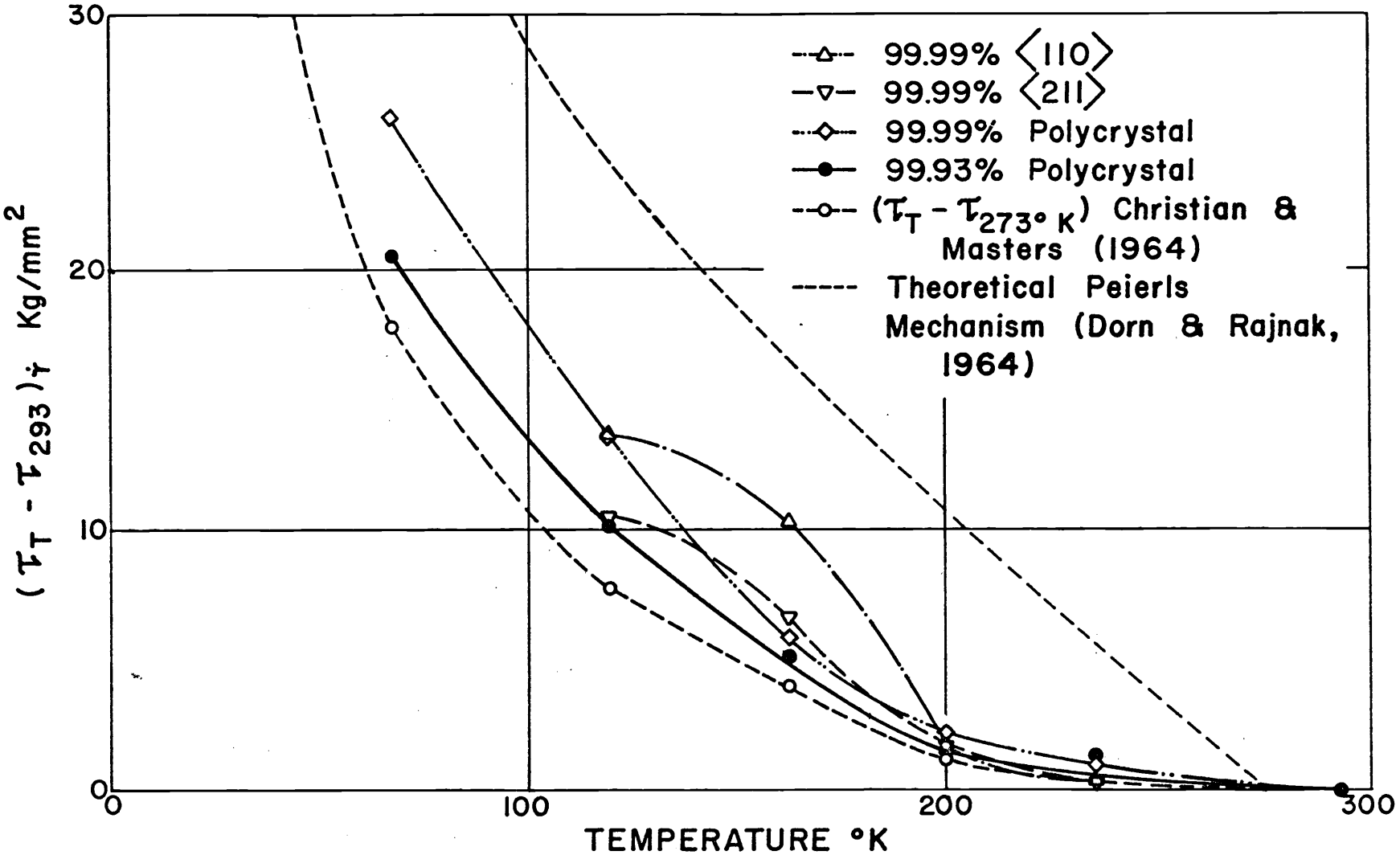

Fig. 19: Resolved flow stress of vanadium versus temperature. ⟨110⟩ or ⟨211⟩ designates tensile axis of specimen.

of changes in slip system with orientation of the tensile axis was considered. However, calculations show that for both the <110> and <211> crystals, the resolved shear stress on $\{211\}$ planes is higher than that on $\{110\}$ planes; the ratio is 1.16 to 1 for the former case and is 1.035 to 1 for the latter. The orientation dependence of flow stress will be discussed in a later section.

The increase of stresses just below 200°K for the lower purity material, 99.93% polycrystals, is a moderate one. This is probably due to the interference of the low temperature deformation mechanism with that at the neighborhood of ambient temperature, which is mainly controlled by the interaction of impurities and dislocations as will be discussed in a later section.

The similarity between the flow stress-versus-temperature and that for the yield stress-versus-temperature curves probably is an indication that the rate controlling mechanisms at different temperature ranges for both types of stress are the same.

The strain rate sensitivity of vanadium versus temperature plot is shown in Fig. 20. where the rate sensitivity is expressed as the difference in stress due to change of strain rate at constant temperature divided by the difference of the natural logarithms of

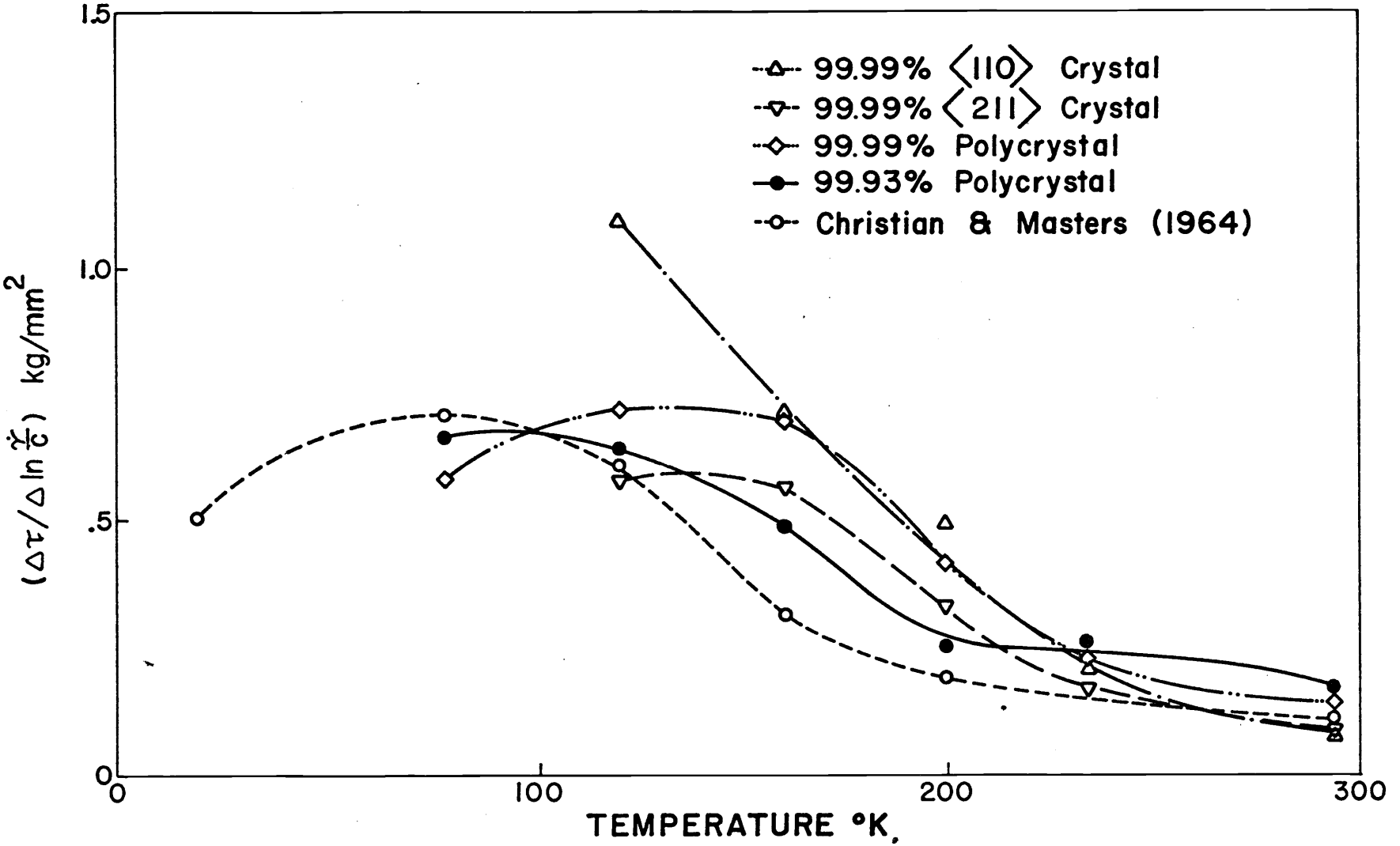

Fig. 20: The strain rate sensitivity of vanadium versus temperature. ⟨110⟩ or ⟨211⟩ designates tensile axis of specimen.

strain rates. The same explanation applied to Fig. 18 and 19 applies also to Fig. 20 except that the sharp increase in sensitivity started at 200°K instead of below that temperature. This is because changing from a lower strain rate to a higher rate is equivalent to a change in the operating temperature from 200°K to a lower temperature at constant strain rate. The sensitivity to the strain rate increases with the purity of the material. Hence the increase is more drastic in the neighborhood of 200°K for 99.99% material than for 99.93% material. At 120°K and lower temperatures the sensitivity still persists, but the increase in stress with decreasing temperature is very great. A given difference of strain rate change is equivalent to a smaller difference of temperature change at this temperature than at higher temperatures. Therefore, the strain rate sensitivity tends to curve down at this temperature range for most materials.

According to Equation (9), the activation enthalpy or the heat of activation has been calculated (Appendix IV) and plotted against temperature in Fig. 21, in which data from Christian and Masters (1964) and Conrad and Hayes (1963) are also shown. The difficulty involved in the determination of the activation enthalpy is mainly due to the difficulty in measuring the exact

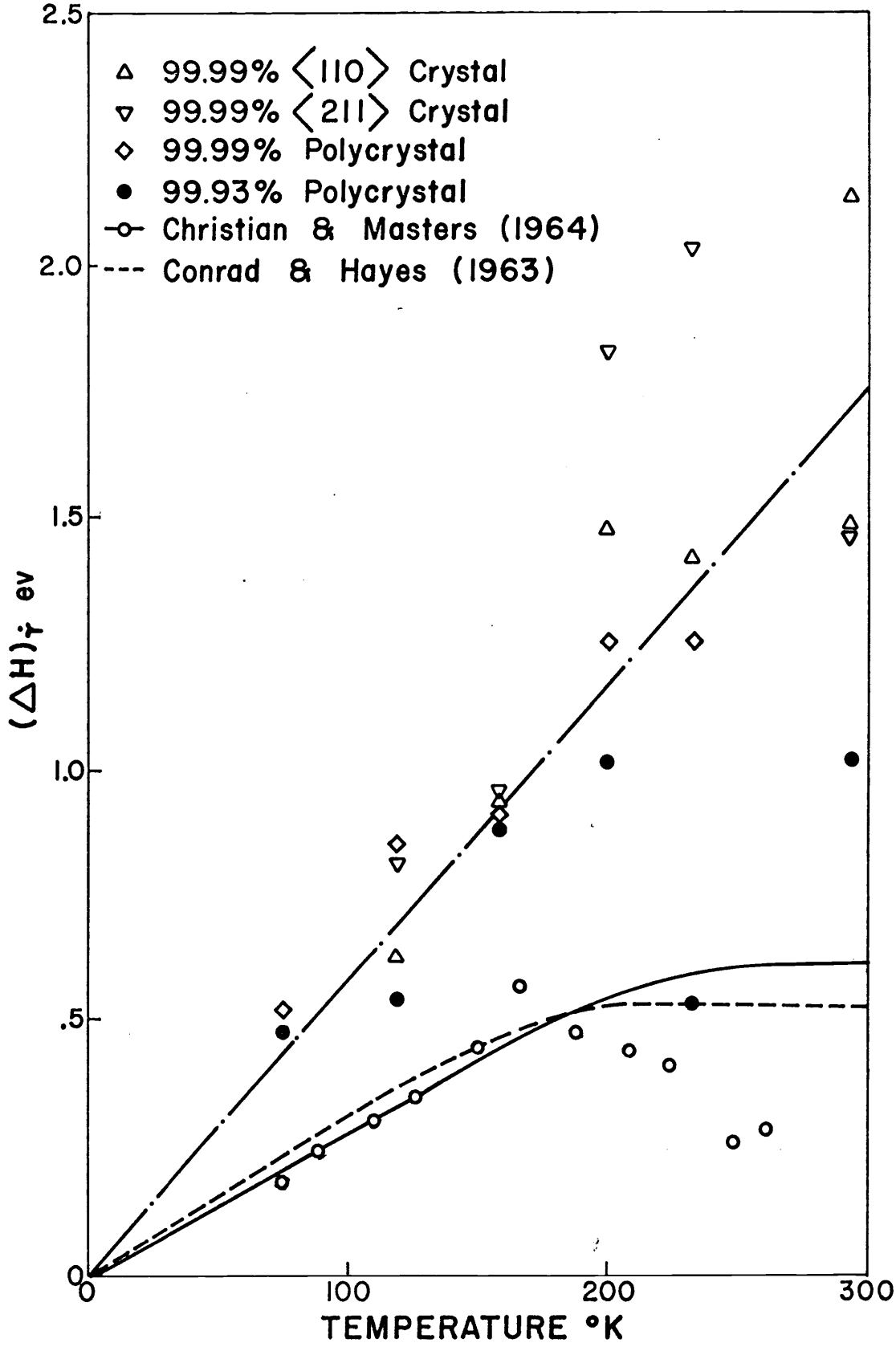

Fig. 21: Activation enthalpy of vanadium versus temperature. ⟨110⟩ or ⟨211⟩ designates tensile axis of specimen.

slope of the effective stress versus temperature curve at a constant strain rate (Fig. 19). More data points are required in order to improve the results of measurements.

The agreement between the present work and previous investigations at temperatures below 200°K was fairly good, considering that different purity grades of vanadium were used. The divergence of the value at temperatures between 200 and 293°K may be, at least partially, due to experimental or calculational error. When both strain rate sensitivity and slope of shear stress versus temperature plot at constant strain rate are small, it is very difficult to calculate ΔH (Appendix IV). Nevertheless, this might indicate a change of rate controlling mechanism occurring at approximately 200°K.

The activation volume has been calculated according to Equation (10) (Appendix IV) and plotted against temperature and effective shear stress in Fig. 22 and 23. The unit of activation volume used in these figures is $\frac{\Delta V}{b^3}$, where b is the magnitude of the Burgers Vector. Except at temperatures above 200°K or when the effective shear stress is very small, all data seem to fall into one curve in each figure, and the agreement of present work and that of Christian and Masters is remarkable. It is apparent that the activation volume is a function of temperature and effective

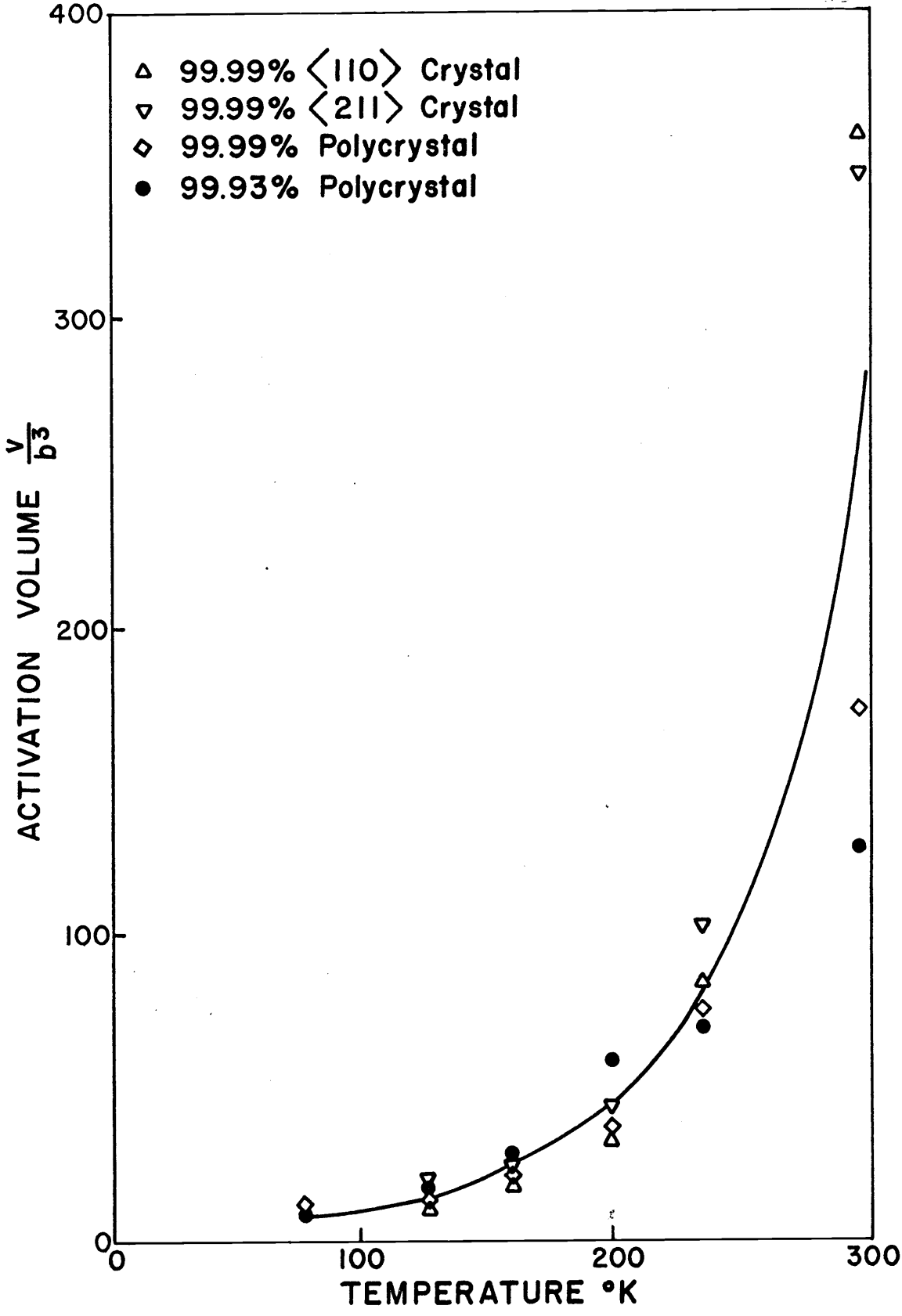

Fig. 22: Activation volume of vanadium versus temperature. ⟨110⟩ or ⟨211⟩ designates tensile axis of specimen.

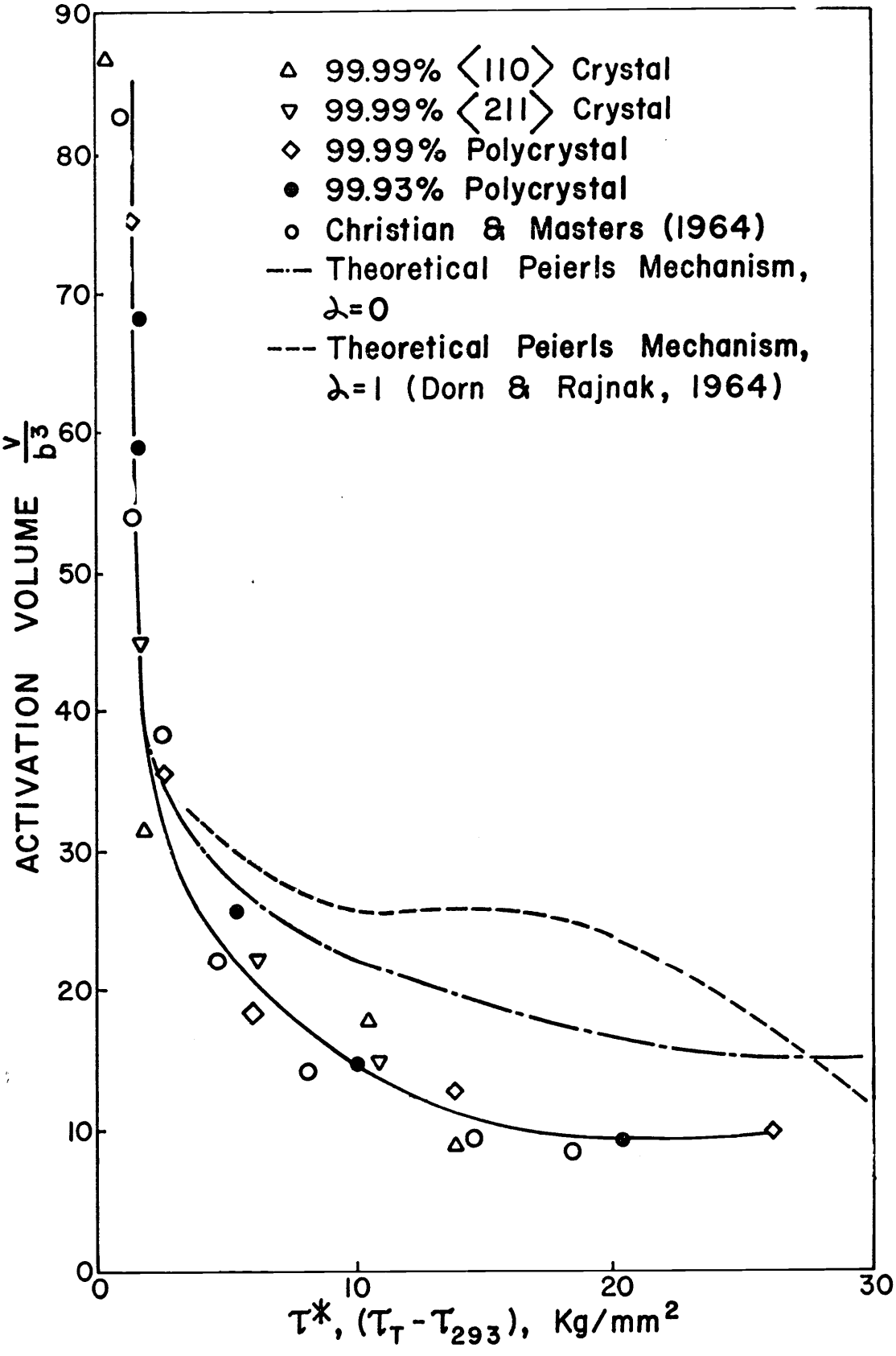

Fig. 23: Activation volume versus effective shear stress of vanadium. ⟨110⟩ or ⟨211⟩ designates tensile axis of specimen.

shear stress.

In the evaluation of enthalpy and volume of activation, it was assumed that the effective shear stress equals the shear stress at the specific temperature minus that at 293°K. This is equivilant to the suggestion that the thermal component of the applied shear stress is zero at and above 293°K. The choice of this critical temperature is somewhat arbitrary. Conrad and Hayes (1963) used 450°K for this temperature; Dorn and Rajnak (1964) used 273°K; Christian and Masters (1964) selected the temperature of 250°K. However, the stress change in the neighborhood of ambient temperature is very small for 99.99% material and no significant consequences are expected by the difference of selection. On the other hand, for lower purity, 99.93%, material, different choices of the critical temperature would give somewhat different results.

VI. DISCUSSION OF RESULTS

(A) Slip and Twinning Systems

Since there are no controversial points of view as to the shear direction and the plane of twinning in BCC metals the twinning systems $\{211\}\langle 111\rangle$ are presumed correct.

Although no general agreement has been reached for slip planes for BCC metals, a theory that the slip system is orientation dependent seems to be a more satisfactory one than others (Foxall, Duesbery and Hirsch, 1967; Bowen, Cristian and Taylor, 1967). These investigators discovered that there was a discrepancy between the theoretical orientation dependence of the operative slip plane and that observed. The results of tensile experiments deviated in the opposite way to those in compression, which was attributed to the asymmetric nature of the slip directions in the $\{211\}$ planes. The asymmetry of slip increases with decreasing temperature. However, the slip planes observed were predominantly of the $\{110\}$ or $\{211\}$ type.

In vanadium, Greiner and Boulin (1967) found that the slip plane was $\{211\}$ in their bending and compression tests in single crystals of $\langle 110\rangle$ direction. The tensile axis of vanadium single crystals used by Mitchell, Fields and Smialek was at the center of the stereographic triangle and the slip plane observed was $\{110\}$. All these results

are in agreement with the theoretical orientation dependence and with the results of Foxall, Duesbery and Hirsch (1967) in niobium single crystals.

The theoretical slip plane for a <211> crystal should be {211}, but it was on the border line between {110} and {211} according to the systematic observations in niobium crystals mentioned above. However, the shear stress resolved in both planes is approximately the same as mentioned above; the resolved shear stress calculated on the {211} plane as was applied in the present work would cause no serious error.

(B) Yield Phenomena

The yield strength at 293°K for vanadium was strongly dependent on the interstitial content of the material. Although only slight yield drops were observed for some of the specimens, it was a general phenomenon that the yield point for lower purity material was a sharp one while that for the higher purity material was a gradual transition from elastic to plastic deformation. The yield drop was noticed for a 99.93% polycrystal even at a low temperature of 160°K, while there was no such drop for a 99.99% <110> crystal at the same temperature or lower. Cottrell locking is dominant at ambient temperature and for lower purity materials, but the effect is relatively slight at lower temperatures and for higher purity materials.

In general, the yield phenomina might be stated as follows: During the initial loading of the specimen, some dislocations are torn from their Cottrell atmosphere. As the stress is increased, the mobility of the dislocations increases and some multiplication occurs by the double cross slip mechanism. For a high purity specimen, the pinning of dislocations is ineffective, the multiplication takes place gradually as strain hardening proceeds.

The orientation and temperature dependence of yield stress was found by Rose, Ferriss and Wulff (1962) in tungsten and by Bowen, Christian, and Taylor (1967) in niobium. Their curves at various temperatures were similar to some of the curves of the present work. High yield stresses and little work hardening were the common characteristics of the stress strain curve for <110> crystals.

(C) Rate Controlling Mechanism of the Activation Process at Low Temperatures

Due to an abrupt change of yield and flow stresses and the strain rate sensitivity at approximately 200°K, at and above which the activation enthalpy changes to a great extent, it is strongly believed that a change of controlling mechanism takes place at this temperature. It is also clear from the present work that the effect

of impurities is great at temperatures above 200°K, substantiated by the well established observations that the resolved flow stress is proportional to the total interstitial content of vanadium at ambient temperature (Reed, 1970). The rate controlling mechanism at temperatures above 200°K is probably the interaction between dislocations and impurities.

The rate controlling mechanism at low temperatures for BCC metals has been studied by many investigators and catagorized in the following (Conrad, 1961):

1. Interaction between dislocations and impurities,
2. Intersection of dislocations;
3. Nonconservative motion of jogs in screw dislocations;
4. Overcoming of the Peierls stress;
5. Cross slip of screw dislocations.

According to the results mentioned above the differential flow stress and strain rate sensitivity are even higher for 99.99% material than that of 99.93% material at temperatures below 200°K. It is apparent that the deformation mechanism controlled by the interaction between dislocations and impurities is not effective. Of the last four mechanisms mentioned above, the intersection of dislocations, or cutting of the forest, can also be eliminated. This is because the experimental volume of

activation is in the range of 8 to 30 b^3, while that expected for this mechanism is several orders of magnitude greater (Seeger, 1954). Furthermore, if it were this mechanism controlling, the difference of shear stress due to change of strain rate should have increased with the increasing of strain and the activation volume should have decreased with the increasing of strain (Conrad and Schoeck, 1960; Conrad, 1961). Both of these did not occur.

Comparing the enthalpy and volume of activation of the last three mechanisms mentioned above with those obtained from the present experiments, they all seem comparable to each other. However, the supporters for the nonconservative motion of jogs in screw dislocations (Schoeck, 1961; Rose, Ferriss and Wulff, 1962) revealed that the activation enthalpy was about 1.5 ev, being half of the self diffusion energy, and the distance between jogs was approximately 50b. According to Eq. (12), $\Delta V = b l d^*$ the activation volume will be approximately $50b^3$, supposing the distance of activation, d^*, is of the magnitude of b. This is slightly greater than the results of the present investigation; also the enthalpy of activation is greater than the value of the experiments at the temperatures between 77°K and 200°K, 0.5 to approx-

imate 1.0 ev.

There were no serious calculations of the activation enthalpy for the cross slip mechanism and that of overcoming Peierls stress (Conrad, 1961), but the dislocation segment involved in the thermal activation (Seeger, 1956; Schoeck and Seeger, 1958) has been found to be in the range of 10 to 50b in both cases. Therefore, the activation volume for both mechanisms is approximately 10 to $50b^3$, which is in agreement with the results of the present experiments. Johnston and Gilman (1959) and Schoeck (1961) claimed the cross slip mechanism was rate controlling for yield as well as flow for BCC metals while Conrad (1961) and Christian and Masters (1964) supported the idea of the Peierls mechanism. However, the recent development in the theory of slightly dissociated screw dislocations in BCC metals (Duesbery and Hirsch, 1968; Dorn, 1968) seems to favor the mechanism based on the cross slip of screw dislocations model over others.

It is believed, in the dissociation model, that the core energy of a screw dislocation is decreased slightly by a minor separation of its partials rather than assuming that a true stacking fault is present. This implies that before such a mildly dissociated screw dislocation can cross slip, its core energy must be

increased somewhat. Such a screw dislocation will then exhibit a periodic variation in energy as it is displaced and behave like one moving to overcome the energy hills of the Peierls mechanism.

The differences between the true Peierls mechanism and the dissociation model, i.e., pseudo-Peierls mechanism are: (1) The former applies to any dislocation in any orientation parallel to close-packed rows of atoms on the slip plane, the latter applies only to dislocations in screw orientation that dissociate very little on secondary planes. The orientation dependence of the flow stress can be explained in the latter mechanism. (2) The former is expected to be operative in the early stages of straining; some prestraining is required to place dislocations in screw orientation before the latter can be controlling. The rate of strain hardening is expected to be high in the early stage of straining.

In view of the fact that the edge components of dislocation loops move considerably faster than the screw components in BCC crystals (Johnston and Gilman, 1959) and that the present investigation shows an orientation dependence of shear stress and a high rate of strain hardening in the early stage of straining, the pseudo-Peierls mechanism is most probably to be the rate

controlling mechanism at temperatures below 200°K.

The overall stress versus temperature picture is depicted in Fig. 24, where T_{c_p} is the critical temperature, above which the thermal stress to overcome the pseudo-Peierls stress is zero. T_{c_I} is the equivalent for overcoming the interaction energy between dislocations and impurities. For high purity vanadium, the former is probably 200°K and the latter, 300°K. However, these critical temperatures are overshadowed by the interaction mechanism for low purity materials as also shown in the figure. This is the difficulty encountered in evaluating the deformation mechanism by using low purity materials.

Dorn and Rajank (1964) have developed a theoretical model for the Peierls mechanism, which should apply both to the true Peierls as well as the Pseudo-Peierls mechanisms mentioned above. They assumed that the energy, $\Gamma(y)$, per unit length of a dislocation line in the direction y, perpendicular to the dislocation with a period "a", the space between parallel rows of close-packed atoms on the slip plane, was approximated by

$$\Gamma(y) = \frac{\Gamma_c + \Gamma_o}{2} + \frac{\Gamma_c - \Gamma}{2}\left(\frac{\alpha}{2} + \cos\frac{2\pi y}{a} - \frac{\alpha}{4}\cos\frac{4\pi y}{a}\right) \qquad (16)$$

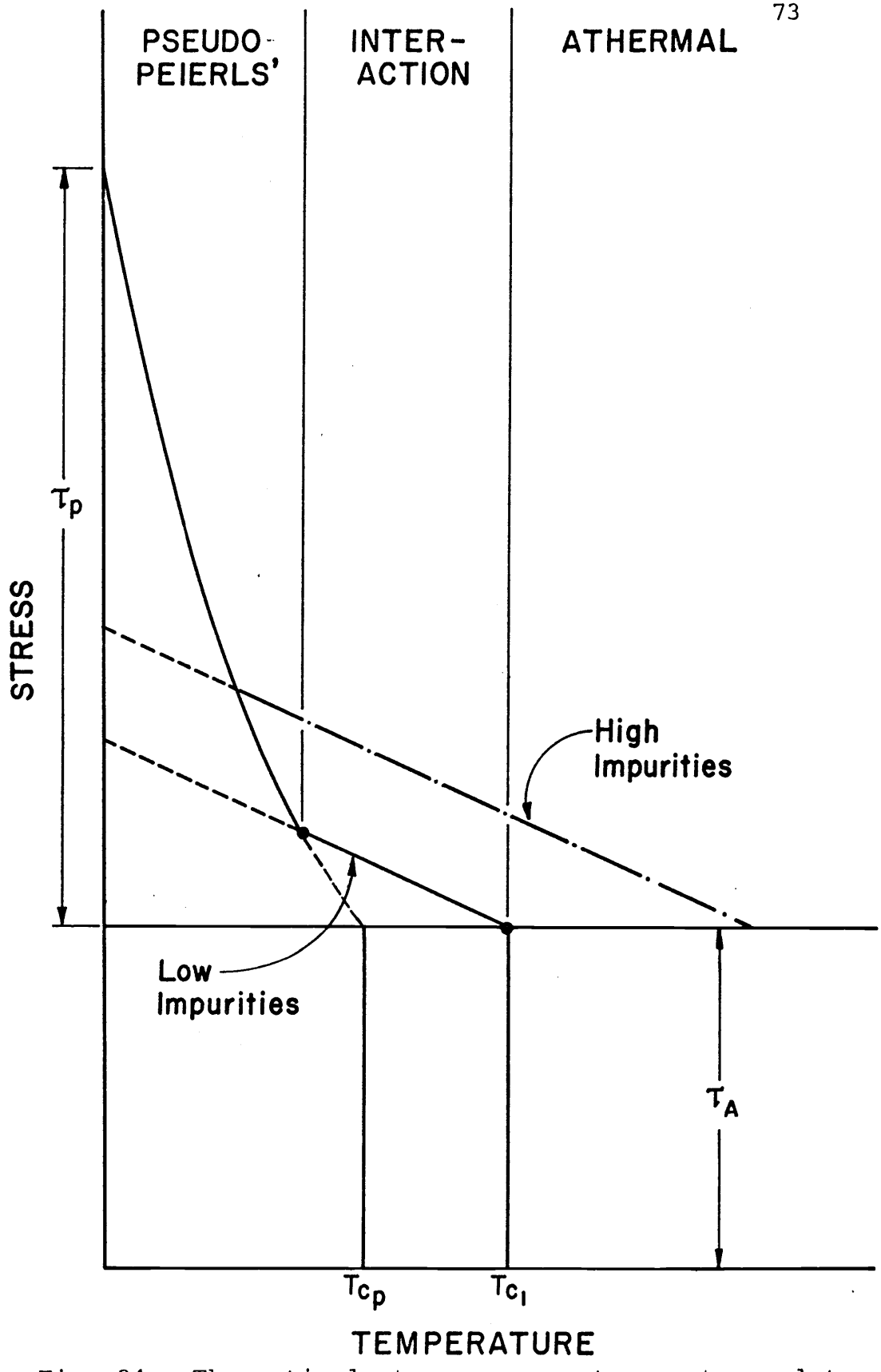

Fig. 24: Theoretical stress versus temperature plot for BCC metals at low temperatures.

where Γ_c and Γ_o are the energies per unit length of a dislocation lying at the top and bottom of the Peierls hill respectively, and α is a factor that varies between -1 and 1. By extensive mathematical manipulations, they obtained the following equations:

$$\frac{\tau_p}{2\Delta U_k}\frac{\partial \Delta U_n}{\partial \tau^*} = \frac{\tau_p}{2U}\Delta V^* \tag{17}$$

and

$$\frac{\Delta U_n}{2\Delta U_k} = \frac{T}{T_{c_p}} \tag{18}$$

Where τ_p is the Peierls stress at 0°K, τ^* effective shear stress, ΔU_k is the enery for a kink in a dislocation line and ΔU_n, the energy to nucleate a pair of kinks, which is assumed to be the process for the dislocation line to move over the Peierls hill. T in Eq. (18) is the experimental temperature and T_{c_p} is the critical temperature, above which the effective shear stress, τ^*, is zero.

There are theoretical curves for effective shear stress, τ^*/τ_p versus left side terms of Eq. (17) and (18). By plotting the empirical curves of effective shear stress versus right side terms, the theoretical and empirical plots can easily be compared. The theoretical activation volume versus effective shear stress curve is shown with the empirical results of vanadium in Fig. 23, and the equivalent plots for activation enthalpy versus shear stress are shown in Fig. 25, assuming T_{c_p} is 200°K. (Appendix IV)

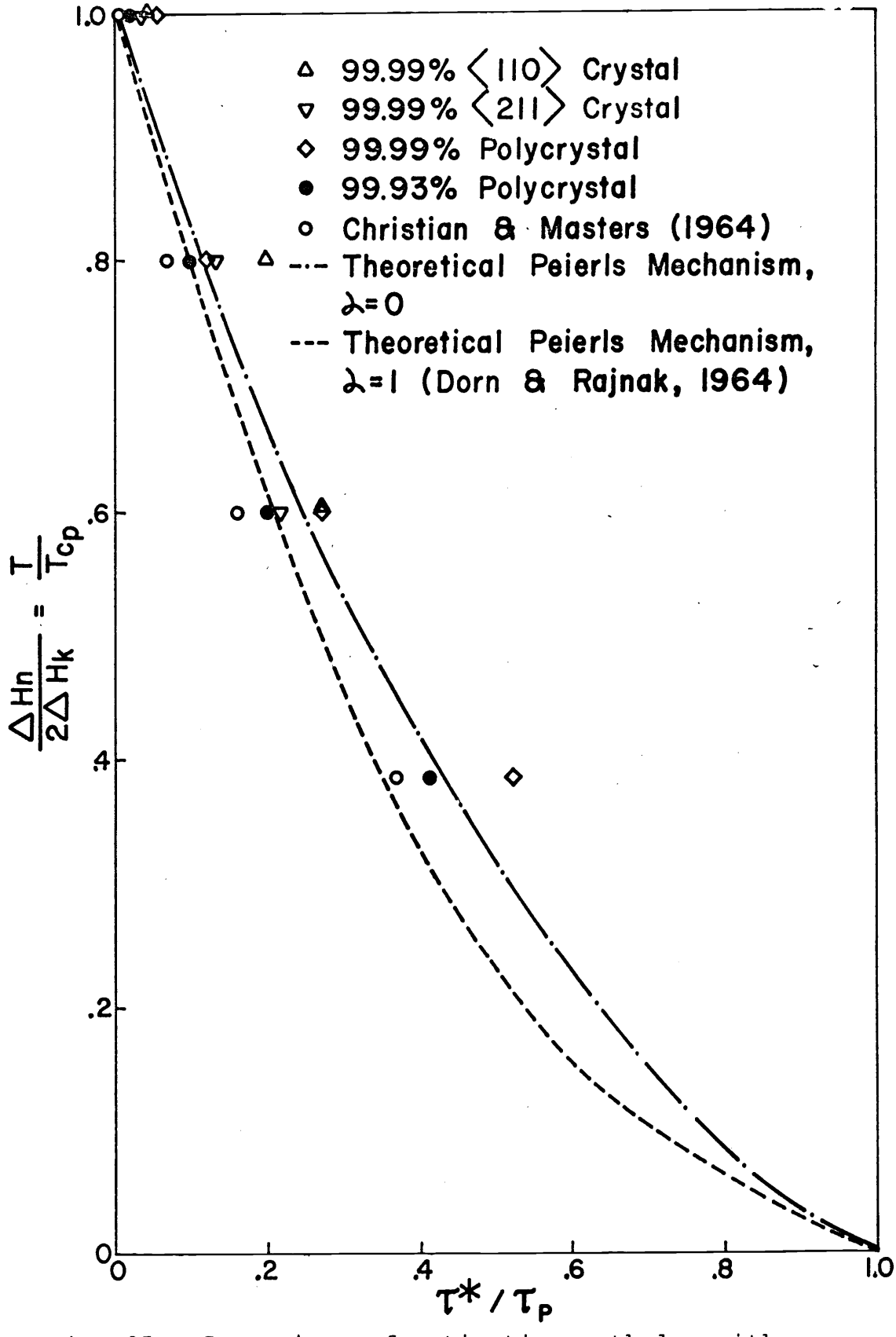

Fig. 25: Comparison of activation enthalpy with theoretical energy to overcome Peierls stress. ⟨110⟩ or ⟨211⟩ designates tensile axis of specimen.

The agreement between the theory and the experimental results is fairly good considering that the possible effects of interstitials on the mechanism were neglected and that other simplifications were made in the theory. The theoretical stress τ versus temperature T, curve presented by Dorn and Rajnak (1964) is also shown with empirical results in Fig. 19. However, this was based on the assumption that T_{c_p} is 273°K. If the assumed T_{c_p} is 200°K, the theoretical curve will shift to the left and agree with the curves for 99.99% vanadium very well.

Some remarks on the activation equation (3), are in order. Since the plot of activation enthalpy at constant strain rate versus temperature is a straight line below 200°K (Fig. 21), the assumption that C is independent of stress and temperature is justified in this range. It is a poor approximation at temperatures above 200°K. The assumption that the enthalpy of activation is a function of temperature and effective shear stress is justified. The relation between activation enthalpy and effective shear stress is generally expressed as $\Delta H = \Delta H^{*} - \Delta V^{*}\tau^{*}$ (Conrad, 1961). In the neighborhood of 200°K, however, there is more than one single mechanism controlling, and the enthalpy data based on a single activation process may not be quite accurate.

(D) Comparison of Testing Materials

The very high purity material, 99.99% vanadium, seems to demonstrate the following characteristics in general: (1) Very fine or indistinct slip lines were observed. This is probably due to the fact that the slip bands are so closely spaced that no slip lines could be observed. (2) It is very ductile even at 77°K. This is contrary to some of the previous observations that vanadium was brittle at low temperatures. (3) The higher the purity of the metal, the greater will be the tendency for twinning. Some tensile specimens twinned at 120°K in the present investigation as compared to a 20°K in a previous investigation (Lindley and Smallman, 1963). (4) The effect of impurities on the flow stress for high purity metal is slight so that the deformation mechanism at low temperatures could be distinguished from that at ambient temperature. A dividing line between the two mechanisms at 200°K is recognized for the first time.

Comparing 99.99% purity <110> single crystals with <211> crystals, an orientation dependence of flow stress has been established which helps to identify the rate controlling mechanism at temperatures below 200°K.

Comparing single crystals and polycrystals of similar purity 99.99% vanadium, the differences in yield,

flow stresses and the strain rate sensitivity were less pronounced than that between single crystals of differing orientation. This is the equivalent of saying that the effect of grain size is a minor one, which is the characteristic of the Peierls or pseudo-Peierls mechanism where the activation volume is tiny as compared to the metallographic grain sizes.

(E) Suggestions for Future Investigations

In view of the experimental results obtained in the present work, the following recommendations are suggested for future investigations in the field of deformation mechanisms for BCC metals at low temperatures.

1. Very high purity metal should be used in order to avoid interference from the effects of impurities. Using different grades of purity of the same metal is desirable for comparison purposes, but the impurity content should be a single element or interstitial alone at various levels.

2. More closely spaced data are required to obtain more accurate evaluations, especially in the calculations for activation enthalpy.

3. Larger temperature ranges should be covered, for instance from 4°K to 400°K, if the difficulties due to twinning and necking down can be overcome.

4. More accurate chemical and analytical techniques are needed so that the exact impurity content is known and the evaluation of the results will not mislead due to inaccurate information.

5. More precise and accurate equipment will facilitate the type of experiments used in the present work and give better results. For example, a stress-strain recorder of very high magnification is required so that the differential change of stress can be accurately recorded. Another apparatus improvement would be a specially built coolant container which permits rapid changes of temperature.

VII. CONCLUSIONS

(A) Mechanical twins are formed in tensile testing of <110> and <211> single crystals of 99.99% purity vanadium at 77°K and 120°K. Twins occur on {211} planes.

(B) In general, slip lines could not be identified on 99.99% vanadium single crystals. The slip plane determined on a <110> single crystal deformed at 160°K by tension is {211}.

(C) 99.99% purity vanadium single crystals deformed at temperatures from 77°K to 293°K generally show a chisel edge type of ductile fracture.

(D) The yield and flow stresses of vanadium are affected to a great extent by impurities at temperatures between 200°K and 293°K, but are little affected at temperatures between 77°K and 200°K.

(E) The resolved flow stresses of single crystals of 99.99% purity vanadium are dependent on orientation.

(F) There is an apparent change of rate controlling mechanism at approximately 200°K on the basis of an abrupt change of yield and flow stresses, the strain rate sensitivity, the activation volume and activation enthalpy at this temperature. The change for 99.99% purity vanadium is remarkable but for 99.93% metal it is less distinct.

(G) The rate controlling mechanism for the deformation of high purity vanadium at temperatures between 200°K and 293°K is most likely the interaction between dislocations and impurities. At temperatures below 200°K, the deformation is probably controlled by slightly dissociated screw dislocation model, i.e., the pseudo-Peierls mechanism.

BIBILIOGRAPHY

1. Atkinson, R.H. and Staff. 1960. Physical metallurgy of tungsten and tungsten alloys. 233p. (U.S. Air Force Contract No. AF 33(616)-5632, WADD-TR-60-37)

2. Avery, D.H., M.L., Ebner and W.A. Backofen. 1958. Electroshaping of copper single crystals. Transactions of the Metallurgical Society of the AIME 220:256

3. Barrett, C.S. Structure of metals, 1966. 3d ed. New York, McGraw-Hill Book Co. 654p.

4. Barrett, C.S., G. Ansel and R.F. Mehl. 1937. Slip. twinning and cleavage in iron and silicon ferrite. Transactions of American Society for Metals 25: 703-736.

5. Barrett, C.S., and R. Bakish. 1953. Twinning and cleavage in tantalum. Transactions of the AIME 212: 122-123.

6. Bolef, D.I. 1961. Elastic constants of single crystals of the bcc transition elements V, Nb and Ta. Journal of Applied Physics 32: 100-105.

7. Bowen, D.K. and J.W. Christian. 1965. The calculation of shear stress and shear strain for double glide in tension and compression. Philosophical Magazine, ser. A, 12: 369-378.

8. Bowen, D.K. J.W. Christian and G. Taylor. 1967. Deformation properties of niobium single crystals. Canadian Journal of Physics 45:903-938.

9. Bradford, S.A. and O.N. Carlson. 1962. Effect of oxygen on the lattice constant, hardness and ductility of vanadium. Transactions of the American Society for Metals 55: 169-178.

10. Calnan, E.A. and C.J.B. Clews. 1951. The development of deformation texture in metals, Part II: Body-centered cubic metals. Philosophical Magazine, ser. 7, 42:616-635.

11. Carlson, O.N. and C.V. Owen. 1961. Preparation of high-purity vanadium metal by the iodide refining process. Journal of Electrochemical Society 108: 88-93.

12. Carlson, O.N., F.A. Schmidt and W.E. Krupp. 1966. A process for preparing high-purity vanadium. Journal of Metals 18:320-323.

13. Christian, J.W. and B.C. Masters. 1964. Low temperature deformation of body-centered cubic metals. Proceedings of Royal Society, (London) A, 281:233-257.

14. Clough, W.R. and A.S. Pavlovic. 1960. The flow, fracture and twinning of commercially pure vanadium. Transactions of the American Society for Metals 52: 948-970.

15. Conrad, 1961. On the mechanism of yielding and flow in iron. Journal of the Iron and Steel Institute 198: 364-375.

16. Conrad, 1964. Thermal activated deformation of metals. Journal of Metals 16: 582-588.

17. Conrad, H. and W. Hayes. 1963. Thermally-activated deformation of the BCC metals at low temperatures. Transactions of the American Society for Metals 56: 249-262.

18. Conrad, H. and G. Schoeck. 1960. Cottrell locking and the flow stress in iron. Acta Metallurgica 8: 791-796.

19. Conrad, H. and H. Wiedersich. 1960. Activation energy for deformation of metals at low temperatures. Acta Metallurgica 8: 128-130.

20. Cottrell, A.H. 1948. Effect of solute atoms on the behavior of dislocations. In: Report of a Conference on Strength of Solids, University of Bristol, July, 1947. London, Physical Society. p. 30-38.

21. Cottrell, A.H. 1958. Theory of brittle fracture in steel and similar metals. Transactions of the AIME 212: 192-203.

22. Cotrell, A.H. 1964. The mechanical properties of matter. New York, John Wiley. 430p.

23. Cottrell, A.H. and B.A. Bilby. 1949. Dislocation theory of yielding and strain aging of iron. Proceedings of Physical Society 62-A: 49-62.

24. Dorn, J.E. 1968. Low-temperature dislocation mechanisms. In: Dislocation dynamics, ed. A.R. Rosenfield et al. Columbus, Ohio, Battelle Memorial Institute. p. 27-55. (Battelle Institute Materials Science Colloquia 1967).

25. Dorn, J.E. and S. Rajnak. 1964. Nucleation of kink pairs and the Peierls mechanism of plastic deformation. Transactions of the Metallurgical Society of AIME 230:1052-1064.

26. Duesbery, M.S. and R.A. Foxall. 1965. Symposium Reinstoffe in Wissenschaft und Technik, Dresden. Cited in: Deformation properties of niobium single crystals, by Bowen, D.K., J.W. Christian and G. Taylor. Canadian Journal of Physics. 45:903-938. 1967.

27. Duesbery, M.S. and P.B. Hirsch. 1968. Effect of core structure on dislocation mobility with special reference to BCC metals. In: Dislocation dynamics, ed A.R. Rosenfield et al. Columbus, Ohio, Battelle Memorial Institute. p. 57-85. (Battelle Institute Materials Science Colloquia, 1967)

28. Edington, J.W. and R.E. Smallman. 1964. The relationship between flow stress and dislocation density in deformed vanadium. Acta Metallurgica 12:1313-1328.

29. Edington, J.W. and R.E. Smallman. 1965. On mechanical twinning in single crystals of vanadium. Acta Metallurgica 13:765-770.

30. Foote Mineral Co., Technical Staff. 1968. Vanadium. In: The Encyclopedia of the Chemical Elements, ed by C.A. Hampel, New York. Reinhold Book Corporation. p. 787-795.

31. Foxall, R.A., M.S. Duesbery and P.B. Hirsch. 1967. The deformation of niobium single crystals. Canadian Journal of Physics 45:607-629.

32. Garlick, R.G. and H.R. Probst. 1964. Investigation of room temperature slip in zone melted tungsten single crystals. Transactions of Metallurgical Society of AIME 230:1120-1125.

33. Gilman, J.J. and W.G. Johnston. 1957. The origin and growth of glide bands in lithium fluoride crystals. In: Dislocations and mechanical properties of crystals, ed. J.C. Fisher et al.. New York, John Wiley & Sons. p. 116-163. (An International Conference, Lake Placid, September 1956).

34. Greiner, E.S. and D.M. Boulin. 1967. The plastic deformation of single crystals of vanadium at 298° and 77°K. Transactions of the Metallurgical Society of AIME 239:965-969.

35. Harding, J. 1969. The effect of grain size and strain rate on the lower yield stress of pure iron at 288°K. Acta Metallurgica 17:949-958.

36. Heslop, J. and N.J. Petch. 1956. The stress to move a free dislocation in alpha iron. Philosophical Magazine. ser. 8, 1:866-873.

37. Hoke, J.H. and R. Maddin. 1956. The deformation of molybdenum single crystals in compression. Journal of Mechanics and Physics of Solids 5:26-40.

38. Honeycombe, R.W.K. 1968. The plastic deformation of metals. New York, St. Martin's Press. 477p.

39. Jaoul, B. and D. Gonzalez. 1961. Deformation plastique de monocristaux de fer. Journal of Mechanics and Physics of Solids 9:16-38.

40. Johnston, W.G. and J.J. Gilman. 1959. Dislocation velocities, dislocation densities and plastic flow in lithium fluoride crystals. Journal of Applied Physics 30:129-144.

41. Kaun, L. A. Luft, J.Richter and D. Schulze. 1965. Symposium Reinstoffe in Wissenschaft und Technik, Dresden. cited in: Deformation properties of niobium single crystals. by Bowen, D.K., J.W. Christian and G. Taylor. Canadian Journal of Physics 45:903-908 1967.

42. Kelly, A. 1953. Neumann bands in pure iron. The Proceedings of the Physical Society A66:403-405.

43. Koehler, J.S. 1952. The nature of work-hardening. Physical Review 86:52-63.

44. Lindley, T.C. and R.E. Smallman. 1963. The plastic deformation of polycrystalline vanadium at low temperatures. Acta Metallurgica 11:361-371.

45. Low, J.R. and R.W. Guard. 1959. The dislocation structure of slip bands in iron. Acta Metallurgica 7:171-179.

46. Maddin, R. and N.K. Chen. 1954. Geometrical aspects of the plastic deformation of metal single crystals. Progress in Metal 5:53-95.

47. McHargue, C.J. 1962. Twinning in Columbium. Transactions of the Metallurgical Society of AIME 224:334-339.

48. Mitchell, T.E., R.J. Fields and R.L. Smialek. 1970. Three-stage hardening in vanadium single crystals. Journal of the Less-Common Metals 20:167-170.

49. Mitchell, T.E. and W.A. Spizig. 1965. Three-stage hardening in tantalum single crystals. Acta Metallurgica 13:1169-1179.

50. Mordike, B.L. 1961. Herstellung von Tantal-Einkristallen durch Elektronenstrahlschmelzen. Zeitschrift fur Metallkunde 52:587-591.

51. Nabarro, F.R. N. and T.R. Duncan. 1967. Dissociated dislocations and the Schmid Law of resolved shear stress in B.C.C. Metals. Canadian Journal of Physics 45:939-943.

52. Orowan, E. 1954. Dislocations and mechanical properties In: Dislocations in metals, ed, by M. Cohen. New York, AIME. Chapter 3.

53. Paxton, H.W. 1953. Experimental verification of twin system in alpha iron. Acta Metallurgica 1:141-143.

54. Petch, N.J. 1953. The cleavage strength of polycrystals. Journal of the Iron and Steel Institute 174:25-28.

55. Pugh, J.W. 1957. Temperature dependence of the tensile properties of vanadium. Transactions of the AIME 209: 1243-1244.

56. Reed, R.E. 1970. Electron beam float zone and vacuum purification of vanadium. Paper presented before the International Vacuum Metallurgy Conference and Third Annual Southwest Section Symposium, American Vacuum Society, Anaheim, California, June 15-19, 1970.

57. Rose, R.M., D.P. Ferriss and J. Wulff. 1962. Yielding and plastic flow in single crystals of tungsten. Transactions of the Metallurgical Society of AIME 224:981-990.

58. Rostoker, W. 1958. The metallurgy of vanadium. New York, John Wiley. 185p.

59. Schadler D.W. 1960. Deformation behavior of zone-melted tungsten single crystals. Transactions of the Metallurgical Society of AIME 218:649-655.

60. Schmid, E. and I. W. Boas. 1968. Plasticity of crystals. London, Chapman and Hall. 353p.

61. Schoeck, G. 1961. On the yield stress in BCC metals. Acta Metallurgica 9:382-384.

62. Schoeck, G. and A. Seeger. 1955. Activation energy problems associated with extended dislocations. In: Report of the Conference on Defects in Crystalline Solids, University of Bristol, July, 1954. London, Physical Society. p. 340-346.

63. Schwartzbart, H. and J.R. Low, Jr. 1949. The yield and strain aging of carburized and nitrided single crystals of iron. Transactions of the AIME 185:637-645.

64. Seeger, A. 1954. Theorie der Kristallplastizität. Zeitschrift fur Naturforschung 9a: 758-775, 856-869.

65. Seeger, A. 1956. On the theory of the low temperature internal friction peak observed in metals. Philosophical Magazine, ser. 8, 1:651-662.

66. Stadelmaier, H.H., W.M. Pritchard and J.E. Grund. 1955. The elastic coefficients of the cubic system with tables for simplified calculation. Raleigh, North Carolina State College, 1955. 9p. (Engineering School Bulleting No. 60)

67. Stein, D.F. 1967. The effect of orientation and impurities on the mechanical properties of molybdenum single crystals. Canadian Journal of Physics 45:1063-1074.

68. Stein D.F. and P.D. Gorsuch. 1961. Etch pit evidence of (112) in iron, Acta Metallurgica 9:904.

69. Sullivan, T.A. 1965. Electrorefining vanadian. Journal of Metals 17: 45-48.

70. Taylor, G. 1965. Doctor of Philosophy Thesis, Oxford, England, Oxford University. Cited in; Deformation properties of niobium single crystals, by D.K. Bowen, J.W. Christian and G. Taylor. Canadian Journal of Physicas 45:903-938. 1967.

71. Taylor, G.I. and C.F. Elam. 1926. The distortion of iron crystals. Proceedings of Royal Society (London), A, 112:337-361.

72. Thompson, R.W. and O.N. Carlson. 1965. Effect of nitrogen and carbon on the low-temperature embrittlement of vanadium. Journal of the Less-Common Metals 9:354-361.

73. Tietz, T.E. and J.W. Wilson. 1965. Behavior and properties of refractory metals, Stanford, California. Standford University Press. 419p.

74. Tsien, L.C. and Y.S. Chow. 1937. The glide of single crystals of molybdenum. Proceedings of Royal Society (London), Ser. A, 163: 19-28.

75. Wang, C.T., E.F. Baroch, S.A. Worcester and Y.S. Shen. 1970. Preparation and properties of high-purity vanadium and V-15Cr-5Ti. Metallurgical Transactions 1:1683-1689.

76. Yaggee, F.L., E.R. Gilbert and J.W. Styles. 1969. Thermal conductivities and densities of vanadium, titanium, chromium and some vanadium base alloys. Journal of the Less-Common Metals 19:39-51.

APPENDICES

APPENDIX I

GROWING SINGLE CRYSTALS BY ELECTRON BEAM FLOAT ZONE REFINING

The electron beam zone refiner is a greatly modified Materials Research EBZ-94 model. It consists of an 18-inch stainless steel bell jar which has a wheeler copper crush gasket seal. All feed-throughs into the chamber are bakeable to 400°C and also have copper gasket flanges. The chamber is baked at 250°C for 16 hours on each pump down cycle. The pumping system is an NRC 10 inch stainless steel diffusion pump which has a water baffle and a liquid nitrogen trap between it and the chamber. The foreline to the 10-inch pump is kept about 1 x 10^{-6} torr pressure during operation by a waterbaffled 4-inch diffusion pump. An activated alumina trap is in the foreline of the 4-inch pump leading to the mechanical pump. After baking, the chamber was at 2-5 x 10^{-9} torr (see records under blank-off pressure). The first pass was often done in 10^{-7} - 10^{-8} torr vacuum but the second pass was in 10^{-9} torr range, sometimes getting on the 10^{-10} torr range.

The electron gun scanner was constructed of stainless steel. The drive screws used ball bearing nuts while the guide rods had linear ball bushings in the moveable cross-heads. The gun used an annular 20 mil tungsten wire about 40mm in diameter for the electron emitter. The tantalum focusing plates were 10mm apart with 25 mm diameter apertures.

The gun was work accelerated with the specimen at high positive potential. The power used for the 1/4 inch diameter vanadium rods was 6000 volts x 36 milliamps or 216 watts. The zoning direction was upward at 10 cm/hr zoning speed. The melt records give most of this latter information for each specimen.

The seed material was Bureau of Mines electrodeposited vanadium for the <110> orientation. The <211> seed was material from the Pratt-Whitney CANEL project. Both of these starting materials had been zone refined prior to making the seeds. There should be little if any impurity pickup from the seeds.

A Veeco GA-4 residual gas analyzer was connected to the system and the most prominent gas during zoning was H_2.

The melt records for vanadium single crystal rods are shown in Table I-1. (Information provided by Dr. R.A. Reed, Oak Ridge National Laboratory, Oak Ridge, Tenn.)

Table I-1 Melting Records of Electron Beam Float Zone Refining of Vanadium

Pass No.	Beam Voltage 1000V	Beam Current AMP	Filament Current AMP	Scan Speed in/hr	Pressure, Torr: Blank off	Pressure, Torr: Start	Pressure, Torr: Finish	Time Hr.
(1) Rod-A, axis of crystal <110>								
1	6	37	11.6	3.9	5.0×10^{-7}	1.0×10^{-7}	3.1×10^{-9}	2:11
2	6	37	11.6	3.9	1.2×10^{-9}	8.5×10^{-10}	1.0×10^{-9}	1:59
(2) Rod-B, axis of crystal <110>								
1	6	34	12.9	3.9	3.9×10^{-9}	7.0×10^{-7}	5.0×10^{-9}	1:58
2	6	34	11.6	3.9	2.5×10^{-9}	1.6×10^{-9}	1.6×10^{-9}	1:49
(3) Rod-C, axis of crystal <110>								
1	6	34	12.0	3.9	1.8×10^{-9}	3.0×10^{-8}	3.5×10^{-9}	2:15
2	6.4	30	14.4	3.9	6.5×10^{-10}	3.0×10^{-9}	2.5×10^{-9}	2:05
(4) Rod-E, axis of crystal <211>								
1	6	37	11.8	3.9	4.4×10^{-9}	5.3×10^{-7}	6.6×10^{-9}	2:05
2	6	37	11.4	3.9	5.0×10^{-9}	4.5×10^{-9}	1.2×10^{-9}	2:00
(5) Rod-G, axis of crystal <211>								
1	6-6.5	35-40	14.0-15.1	3.8	1.7×10^{-9}	2.4×10^{-7}	5.2×10^{-10}	2:10
2	6-6.4	34-37	15.0-15.4	3.8	7.0×10^{-11}	6.5×10^{-10}	1.3×10^{-10}	2:14

APPENDIX II

CALCULATION OF YOUNGS MODULI FOR SINGLE CRYSTALS

Suppose the reference frame for the equations of the theory of elasticity be (x',y',z') and the crystal axis of the cubic system be (x,y,z). According to Stadelmaier, Pritchard and Grund (1955), the elastic coefficients will be functions of the fourth degree of the direction cosines that are defined by the following scheme:

	X	Y	Z
X'	α_1	α_2	α_3
Y'	β_1	β_2	β_3
Z'	γ_1	γ_2	γ_3

Use the following abbreviations:

$$\Omega_\alpha = \alpha_1^2 \alpha_2^2 + \alpha_2^2 \alpha_3^2 + \alpha_3^2 \alpha_1^2 \quad \text{etc.} \tag{19}$$

$$\Omega_{\alpha\beta\gamma} = \Omega_\alpha - \Omega_\beta - \Omega_\gamma \tag{20a}$$

$$\Omega_{\beta\gamma\alpha} = \Omega_\beta - \Omega_\gamma - \Omega_\alpha \quad \text{etc.} \tag{20b}$$

$$C = c_{11} - c_{12} - 2c_{44} \tag{21}$$

Then the constants of the new coordinates are related to the constants of crystal axes as follows:

$$c'_{11} = c_{11} - 2C\,\Omega_\alpha \tag{22a}$$

$$c'_{22} = c_{11} - 2C\,\Omega_\beta \tag{22b}$$

$$c'_{33} = c_{11} - 2C\,\Omega_\gamma \tag{22c}$$

$$c'_{23} = c'_{32} = c_{12} - C\,\Omega_{\alpha\beta\gamma} \tag{23a}$$

$$c'_{13} = c'_{31} = c_{12} - C\,\Omega_{\beta\gamma\alpha} \tag{23b}$$

$$c'_{12} = c'_{21} = c_{12} - C\,\Omega_{\gamma\alpha\beta} \tag{23c}$$

We have, for vanadium (Bolef, 1961)

$$c_{11} = 22.7 \times 10^{11} \text{ dynes/cm}^2 \quad (24a)$$

$$c_{12} = 11.9 \times 10^{11} \text{ dynes/cm}^2 \quad (24b)$$

$$c_{44} = 4.26 \times 10^{11} \text{ dynes/cm}^2 \quad (24c)$$

In the case of an uniaxial tensile stress, the stress-strain equations are as follows:

$$\sigma'_{11} = C'_{11}\,\varepsilon_{11} + C'_{12}\,\varepsilon_{22} + C'_{13}\,\varepsilon_{33} = 0 \quad (25a)$$

$$\sigma'_{22} = C'_{21}\,\varepsilon_{11} + C'_{22}\,\varepsilon_{22} + C'_{23}\,\varepsilon_{33} \quad (25b)$$

$$\sigma'_{33} = C'_{31}\,\varepsilon_{11} + C'_{32}\,\varepsilon_{22} + C'_{33}\,\varepsilon_{33} = 0 \quad (25c)$$

Solving σ'_{22} in terms of ε_{22}, then we obtain the Youngs Modulus for this direction,

$$E_{22} = \frac{\sigma'_{22}}{\varepsilon_{22}} \quad (26)$$

For <110> crystal, X' = [100], Y' = [110] Z' = [$\bar{1}$10] we have,

$$\alpha_1 = 1 \qquad \alpha_2 = 0 \qquad \alpha_3 = 0$$

$$\beta_1 = 0 \qquad \beta_2 = -\frac{1}{\sqrt{2}} \qquad \beta_3 = \frac{1}{\sqrt{2}}$$

$$\gamma_1 = 0 \qquad \gamma_2 = \frac{1}{\sqrt{2}} \qquad \gamma_3 = \frac{1}{\sqrt{2}}$$

Substituting all these values in Eq. (19) and (20) and carry out the calculations from Eq. (22a) through (26), we obtain

$$E_{22} = 1.26 \times 10^4 \text{ kg/mm}^2$$

For <211> crystal, X' = [01$\bar{1}$], Y' = [211], Z' = [1$\bar{1}\bar{1}$]

$$\alpha_1 = \text{Cos } 45°, \qquad \alpha_2 = 0 \qquad \alpha_3 = -\text{Cos } 45°$$

$$\beta_1 = \text{Cos } 65.9°, \qquad \beta_2 = -\text{Cos } 35.26°, \qquad \beta_3 = \text{Cos } 65.9°$$

$$\gamma_1 = \text{Cos } 54.74°, \qquad \gamma_2 = \text{Cos } 54.74°, \qquad \gamma_3 = \text{Cos } 54.74°$$

Applying the same calculations as mentioned above, we obtain

$$E_{22} = 1.27 \times 10^4 \text{ kg/mm}^2$$

APPENDIX III

CALCULATION OF SHEAR STRESS AND STRAIN

(A) For Polycrystals

Let A_o = Original cross sectional area

L_1 = Load in the region where the material is behaving in an essentially eleastic manner. The corresponding strain is $\varepsilon_1 = \frac{L_1}{A_o E}$

where E = Youngs Modulus = 1.3×10^4 kg/mm2

The apparent strain is

$$\varepsilon' = \varepsilon + \frac{e_1}{l_o} = \frac{e}{l_o}$$

where elongations are

$$e_1 = l_f - l_o, \qquad e_1 = l_f - l_1$$

l_1 is the gauge length when the load is L_1 ; l_o and l_f are the original and final gauge lengths respectively.

We have the true strain,

$$\varepsilon = \int_{l_o}^{l_f} \frac{dl}{l} = \ln \frac{l_f}{l_o} = \ln (1 + \varepsilon') \qquad (27)$$

and true stress

$$\sigma = \frac{L}{A_f} = \frac{L}{A_o} \frac{A_o}{A_f} = \frac{L}{A_o} \frac{l_f}{l_o} \qquad (28)$$

$$= \frac{L}{A_o} (1 + \varepsilon')$$

Therefore, the shear stress is

$$\tau = \frac{L}{2 A_o} (1 + \varepsilon') \qquad (28a)$$

(B) For <211> Crystals

For a $[\bar{1}12]$ crystal, slip occurs on $(\bar{2}11)$ $[111]$ and $(\bar{1}21)$ $[\bar{1}\bar{1}1]$ systems.

According to Bowen and Christian (1965)

$$\gamma = 3\sqrt{2} \ln \left[\frac{3 + \sqrt{2} \cot \beta}{3 + \sqrt{2} \cot \beta_o} \right] \quad (29)$$

$$\tau = \frac{L}{A^\circ} \frac{l}{l_o} \frac{\sqrt{11}}{6} \cos \beta \cos (64.77^\circ - \beta) \quad (30)$$

where $\beta_o = 35.26^\circ$ is the angle between $[\bar{1}12]$ and $[001]$, $[\bar{1}12]$ is the tensile axis and $[001]$ is the resultant slip direction, and

$$\beta = \sin^{-1} \left[\frac{l_o}{l} \sin \beta_o \right]$$

$$= \sin^{-1} \left[\frac{\sin \beta_o}{1 + \varepsilon'} \right]$$

(C) For <110> Crystals

For a $[011]$ crystal, slip occurs on $(\bar{2}11)$ $[111]$ and (211) $[\bar{1}11]$ systems. The resultant slip direction is $[011]$; no rotation is involved. We have,

$$\tau = \frac{L}{A^\circ} (1 + \varepsilon') \cos 35.26^\circ \cos 54.74^\circ$$

$$= \frac{L}{A^\circ} \frac{\sqrt{2}}{3} (1 + \varepsilon') \quad (31)$$

According to Schmid and Boas (1968),

$$\gamma = \frac{1}{\cos 54.74^\circ} \left[\left\{ \left(\frac{l}{l_o} \right)^2 - \sin^2 \theta_o \right\}^{\frac{1}{2}} - \cos \theta_o \right] \quad (32)$$

Take the derivative,

$$d \frac{l}{l_o} = \cos 54.74^\circ \cos \theta \, d\gamma \quad (33)$$

Here $\theta = \theta_o = 35.26^\circ$. Integrating (33), we have

$$\gamma = \frac{l}{l_o} \cos 54.74^\circ \cos 35.26$$

$$= \frac{3}{\sqrt{2}} \ln (1 + \varepsilon')$$

Alternative Method (Bowen and Christian, 1965)

$$\tau = \frac{L}{A_o} \frac{\ell}{\ell_o} \frac{\sqrt{2}}{3} \cos^2 \beta \qquad (35)$$

$$\gamma = \frac{3}{\sqrt{2}} \ln \frac{\cot \beta}{\cot \beta_o} \qquad (36)$$

Where

$$\sin \beta = \frac{\ell_o}{\ell} \sin \beta_o$$

$$\cos \beta = \left\{ \frac{\ell^2 - \ell_o^2 + \ell_o^2 \cos^2 \beta_o}{\ell^2} \right\}^{1/2}$$

Here

$$\beta_o = 0 \quad , \quad \beta = 0$$

$$\cos \beta = 1$$

and

$$\frac{\cot \beta}{\cot \beta_o} = \left\{ \frac{\ell^2 - \ell_o^2 (1 - \cos^2 \beta_o)}{\ell^2} \right\}^{1/2} \frac{\ell}{\ell_o} \frac{1}{\sin \beta_o} \frac{\sin \beta_o}{\cos \beta_o}$$

$$= \frac{\ell}{\ell_o} = 1 + \varepsilon' \qquad (37)$$

Substituting (37) in (35) and (36), we have

$$\tau = \frac{L}{A_o} \frac{\sqrt{2}}{3} (1 + \varepsilon')$$

$$\gamma = \frac{3}{\sqrt{2}} \ln (1 + \varepsilon')$$

APPENDIX IV

RAW DATA AND CALCULATIONS

(A) Resolved Yield Stress of Vanadium

Specimen Designation	Purity %	Specimen Type[1]	Strain Rate 10^{-5} Sec^{-1}	Resolved Yield Stress, kg/mm^2	
				Proportional Limit	0.2% Offset
1. 293°K					
13-322	99.93	P.C.	6.50	8.35	8.93
99-223	99.99	P.C.	6.50	3.67	3.80
F-6	99.99	S.C.<110>	6.30	1.48	1.74
G-4	99.99	S.C.<211>	6.41	0.86	1.10
2. 233°K					
13-230	99.99	P.C.	6.67	9.6	10.3
F-6	99.99	S.C.<110>	6.30	2.48	3.10
G-5	99.99	S.C.<211>	7.25	2.70	2.96
3. 200°K					
13-225	99.93	P.C.	6.67	12.80	13.95
99-217	99.99	P.C.	6.67	8.45	8.60
A-1	99.99	S.C.<110>	7.25	4.90	5.32
E-2	99.99	S.C.<211>	6.30	2.54	4.57
4. 160°K					
13-19A	99.93	P.C.	6.67	13.6	14.3
99-218	99.99	P.C.	6.80	11.6	13.4
D-5	99.99	S.C.<110>	6.67	7.28	10.9
G-2	99.99	S.C.<211>	6.18	6.61	8.5

continued on next page

Specimen Designation	Purity %	Specimen Type	Strain Rate 10^{-5} Sec^{-1}	Resolved Yield Stress, kg/mm^2	
				Proportional Limit	0.2% Offset
5. 120°K					
13-220A	99.93	P.C.	6.67	16.7	18.1
99-226	99.99	P.C.	6.53	17.1	19.5
D-4	99.99	S.C.<110>	7.11	12.7	17.5
E-4	99.99	S.C.<211>	6.3	10.7	12.0
6. 77°K					
13-322	99.93	P.C.	6.53	22.4	29.2
99-222	99.99	P.C.	6.67	32.4	33.1

Notes: (1) P.C.: Polycrystals; S.C.: Single Crystals; <110>, <211> are orientations of tensile axis.

(2) For polycrystals, assuming $\tau = 0.5\sigma$.

(3) All yield stresses for temperatures below 293°K were obtained after prestraining for about 2% at 293°K.

(4) 0.2% offset values were used for plotting (Fig. 18).

(B) Calculations of Activation Enthalpy

$A = -\left(\frac{\partial \tau^*}{\partial T}\right)_{\dot{\varepsilon}}$ kg/mm²·°K, $B = \left(\frac{\partial \tau^*}{\partial \ln \dot{\varepsilon}}\right)_T$ kg/mm²

$k = 1.38 \times 10^{-16}$ erg/°K $= 8.62 \times 10^{-5}$ ev/°K

$\Delta H = kT^2 (A/B)$ ev

T°K	293	233	200	160	120	77
$T^2, 10^{-4}$	8.59	5.43	4.00	2.56	1.44	0.593
KT^2	7.396	4.680	3.448	2.207	1.241	0.511
	1. For 99.93% Polycrystals					
A	0.024	0.030	0.084	0.192	0.280	0.600
B	0.174	0.261	0.261	0.478	0.634	0.651
A/B	0.138	0.115	0.322	0.402	0.442	0.921
ΔH	1.020	0.538	1.110	0.887	0.549	0.471
	2. For 99.99% Polycrystals					
A	0.026	0.064	0.160	0.284	0.480	0.594
B	0.1302	0.239	0.434	0.686	0.708	0.586
A/B	0.200	0.268	0.368	0.414	0.678	1.013
ΔH	1.479	1.254	1.269	0.914	0.841	0.518
	3. For 99.99% <110> Crystals					
A	0.018	0.064	0.210	0.296	0.560	
B	0.063	0.208	0.491	0.695	1.094	
A/B	0.286	0.307	0.428	0.426	0.512	
ΔH	2.120	1.437	1.476	0.940	0.635	
	4. For 99.99% <211> Crystals					
A	0.013	0.075	0.185	0.240	0.380	
B	0.065	0.174	0.347	0.556	0.586	
A/B	0.199	0.432	0.533	0.432	0.648	
ΔH	1.472	2.022	1.838	0.953	0.804	

(C) Calculations of Activation Volume

$$B = \left(\frac{\partial \tau^*}{\partial \ln \frac{\dot{\varepsilon}}{\dot{\varepsilon}}}\right)_T \quad kg/mm^2$$

$k = 1.38 \times 10^{-16}$ erg/°K $= 1.41 \times 10^{-22}$ kg-cm/°K

$$\Delta V = kT/B = 1.41 \times 10^{-24} \; T/B \; cm^3$$

For Vanadium

$$b^3 = (2.63 \times 10^{-8})^3 = 18.2 \times 10^{-24} \; cm^3$$

$$\frac{\Delta V}{b^3} = \frac{1.41 \times 10^{-24} T}{18.2 \times 10^{-24} B} = 0.0775 \frac{T}{B}$$

Calculations are shown in Table IV-1

Table IV-1 Calculations of Activation Volume

T	293	233	200	160	120	77
(1) 99.93% Polycrystal						
B	0.174	0.261	0.261	0.478	0.634	0.651
$\Delta V/b^3$	131	69.19	59.4	25.94	14.67	9.167
τ^*	0	1.55	1.60	5.35	10.05	20.50
(2) 99.99% Polycrystal						
B	0.130	0.239	0.434	0.686	0.708	0.586
$\Delta V/b^3$	175	75.55	35.71	18.08	13.14	10.18
τ^*	0	1.12	2.76	6.65	13.8	26.0
(3) 99.99% <110> Crystal						
B	0.0629	0.208	0.491	0.695	1.094	
$\Delta V/b^3$	361	86.81	31.57	17.84	8.50	
τ^*	0	0.55	2.0	10.25	13.8	
(4) 99.99% <211> Crystal						
B	0.0652	0.174	0.347	0.556	0.586	
$\Delta V/b^3$	348	103.8	44.67	22.30	15.87	
τ^*	0	0.55	1.90	7.10	10.8	

Note: $\tau^* = \tau_T - \tau_{293}$ values are obtained from original data; they are listed here for the plot of $\Delta V/b^3$ versus effective shear stress (Fig. 23)

(D) Comparison of Activation Enthalpy With Theoretical Energy to Nucleate a Pair of Kinks (Fig. 24)

Assume $\tau_c = 200°K$, $\tau_p = 50\ kg/mm^2$

$\tau^* = \tau_T - \tau_{293}$

					Material Discription
T°K	77	120	160	200	
T/T_c	0.385	0.60	0.80	1.00	
τ^*		13.8	10.25	2.00	99.99%<110>crystal
		10.8	7.10	1.90	99.99%<211>crystal
	26.0	13.8	6.65	2.76	99.99%Polycrystal
	20.5	10.1	5.35	1.60	99.93%Polycrystal
	18.0	8.0	3.50	1.25	Christian and Masters (1964)
τ^*/τ_p		0.276	0.205	0.040	99.99%<110>crystal
		0.216	0.142	0.038	99.99%<211>crystal
	0.52	0.276	0.133	0.055	99.99%Polycrystal
	0.41	0.202	0.107	0.032	99.93%Polycrystal
	0.36	0.160	0.070	0.025	Christian and Masters (1964)